Temporal characteristics of plankton indicators in coastal waters: High-frequency data from PlanktonScope

Hongsheng Bi, Junting Song, Jian Zhao, Hui Liu, Xuemin Cheng, Linlin Wang, Zhonghua Cai, Mark Benfield, Saskia Otto, Eric Goberville, et al.

Journal of Sea Research 189 (2022) 102283

Contents lists available at ScienceDirect

Journal of Sea Research

journal homepage: www.elsevier.com/locate/seares

Temporal characteristics of plankton indicators in coastal waters: High-frequency data from PlanktonScope

Hongsheng Bi [a,*], Junting Song [b], Jian Zhao [a], Hui Liu [c], Xuemin Cheng [b], Linlin Wang [d], Zhonghua Cai [b], Mark C. Benfield [e], Saskia Otto [f], Eric Goberville [g], Julie Keister [h], Yong Yang [i], Xinglong Yu [i], Jun Cai [i], Kezhen Ying [j], Alessandra Conversi [k]

[a] University of Maryland Center for Environmental Science, Solomons, MD 20688, United States
[b] Tsinghua Shenzhen International Graduate School, Shenzhen, Guangdong 518055, PR China
[c] Texas A& M University at Galveston, Galveston, TX 77553, United States
[d] Water Science and Environmental Engineering Research Center, Shenzhen University, Shenzhen, Guangdong 518060, PR China
[e] Louisiana State University, Baton Rouge, Louisiana 70803, United States
[f] Institute of Marine Ecosystem and Fisheries Science (IMF), Center for Earth System Research and Sustainability (CEN), Hamburg University, Hamburg, Germany
[g] Muséum National d'Histoire Naturelle, Sorbonne Université, Université de Caen Normandie, Université Des Antilles, CNRS, UMR 8067 BOREA, Paris, France
[h] School of Oceanography, University of Washington, Seattle, WA 98195, United States
[i] Yangjiang Nuclear Power C. LTD, Yangjiang, Guangdong, PR China
[j] Oasis Photobio Tech LLC., Shenzhen, Guangdong, PR China
[k] National Research Council, Institute of Marine Science, La Spezia, Italy

ARTICLE INFO

Keywords:
Plankton indicators
PlanktonScope
Image processing
Spatial scale
Temporal scale
Time series
Phytoplankton
Zooplankton
South China Sea
Tide
Diurnal cycle
Monsoon
Typhoon

ABSTRACT

Plankton are excellent indicators of ecosystem status and fisheries because of their pivotal role in marine food webs and their core values in the integrated ecosystem assessment (IEA). Monitoring plankton is essential to understand their dynamics and underlying processes. Recent advances in imaging technologies have enabled in situ, high-frequency, real-time observations of plankton in coastal waters. While high-frequency plankton time series have provided unprecedented fundamental information about physical and biological processes, understanding and identifying the underlying mechanisms that influence plankton dynamic remains a major challenge. We use high-frequency plankton data from PlanktonScope as an example to examine the impacts of physical and biological processes on plankton dynamics at different temporal scales. Frequency patterns were identified for both environmental factors and different plankton groups that matched in time. Using logistic regression models on the selected daily peaks for different plankton groups, we found that diurnal cycle, monsoon season, and major episodic events, such as typhoons, had major impacts on the dynamics of plankton, as proxied by our indicators. We further synthesized, across multiple spatiotemporal scales in the study area, the impacts of various processes on plankton with different mobility. Our study demonstrates that the suite of plankton indicators simultaneously generated from PlanktonScope provides a robust holistic view of pelagic ecosystem status over a broad range of spatiotemporal scales. In situ imaging systems like PlanktonScope are promising tools for near real-time plankton monitoring and a deep understanding of plankton dynamics.

1. Introduction

Estuarine and coastal ecosystems are highly productive and often serve as nursery habitat for important fisheries species (Nagelkerken et al., 2015; Sheaves et al., 2015), but they are among the most threatened natural systems globally (Barbier et al., 2011; Halpern et al., 2008; Lotze et al., 2006). The degradation of estuarine and coastal ecosystems can be caused by many intertwined factors, such as excessive nutrients, pollutants, hypoxia, habitat alteration or loss, and overfishing (Borja et al., 2010). Their degradation often contributes to major ecological and environmental issues, such as harmful algal blooms, macroalgal bloom, jellyfish blooms, and resource depletion (Anderson, 2009; Purcell et al., 1999). Indicators have long been used to detect changes in estuarine and coastal systems (Aubry and Elliott, 2006; Borja

* Corresponding author.
E-mail address: hbi@umces.edu (H. Bi).

https://doi.org/10.1016/j.seares.2022.102283
Received 23 August 2022; Received in revised form 23 September 2022; Accepted 27 September 2022
Available online 28 September 2022

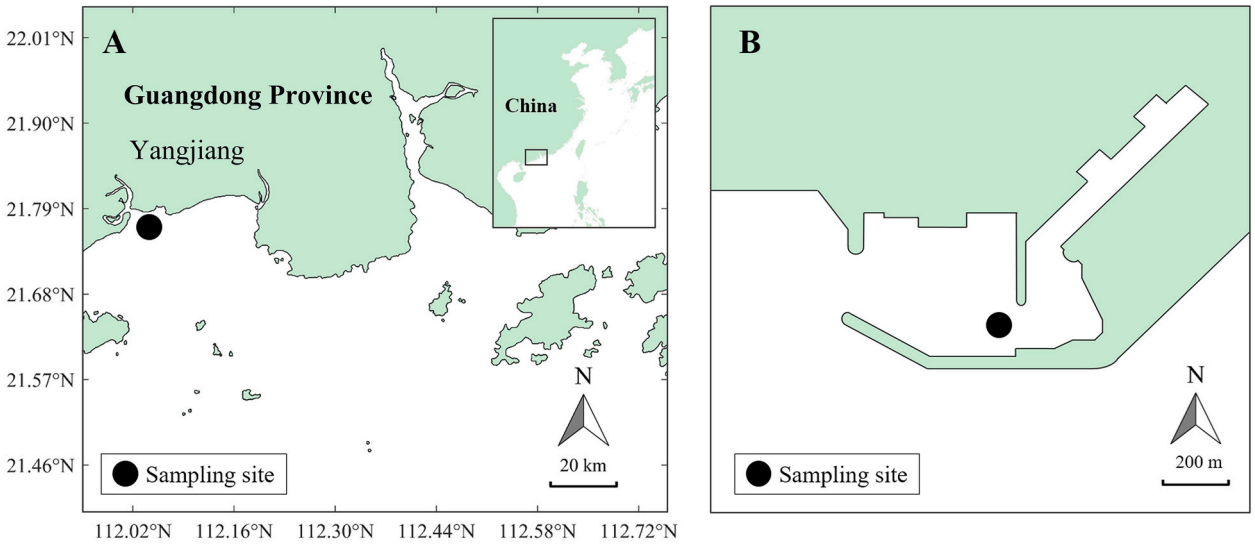

Fig. 1. Study area and sampling site. (A) Study area with the small map in the upper left corner showing the south China coast. (B) Illustration of man-made harbor for cooling water intake.

and Dauer, 2008).

In the past two decades, IEA has become an important framework to formulate policies for fisheries and ecosystem management and restoration (Druon et al., 2019; Heneghan et al., 2020; Levin et al., 2009). A crucial step in IEA is to develop (a suite of) indicators as proxies for key physical and biological processes and to infer the ecosystem status (Dumelle et al., 2021; Harvey et al., 2020; Piet et al., 2008; Shin et al., 2010). Plankton indicators show rapid response to changes in marine ecosystems and are widely used in the assessment of ecosystem status (Beaugrand et al., 2008; Beaugrand and Kirby, 2010; Lomartire et al., 2021; Ndah et al., 2022; Racault et al., 2014). Therefore, plankton indicators are the heart of IEA because of plankton's pivotal roles in food webs and fisheries-plankton interactions (Diekmann et al., 2010; Ndah et al., 2022).

Plankton are a diverse group of organisms defined by their inability to swim actively against a current rather than by biological factors. They not only vary in size - from a few micrometers to several meters - but also in functional traits (Beardall et al., 2009; Litchman et al., 2007; Teodósio and Barbosa, 2022). Phytoplankton are the primary producers and the basis of the marine food chain. Zooplankton are important prey species for juvenile fish, and such interactions have been postulated as the basis for the "Critical Period hypothesis" (Hjort, 1914) and "Match-Mismatch hypothesis" (Cushing, 1969) to explain fish recruitment variation. Some zooplankton species can affect the ecosystem structure disproportionately because they are critical food sources for many top predators, such as krill (Melbourne-Thomas, 2020; Trathan and Hill, 2016), mysids (Feyrer and Duffus, 2015), and some high-nutrient-content copepods like *Calanus finmarchicus* (Heath and Lough, 2007; Huserbråten et al., 2018; Papworth et al., 2016). In recent years, jellyfish (*Cnidaria*) became conspicuous in many ecosystems with rapid outbursts or periodic blooms (Mills, 2001; Purcell et al., 2007; Uye, 2014) and their proliferations often have detrimental effects for fisheries (e.g., Purcell, 1985; Richardson et al., 2009), although beneficial impacts for biogeochemical cycles and ecosystem functioning also exist (Lebrato et al., 2019; Tinta et al., 2021).

Several characteristics of plankton make them excellent indicators (Mackas and Beaugrand, 2010; Mackas et al., 2001; Ndah et al., 2022; Racault et al., 2012). First, plankton are ubiquitous in the ocean, which makes them easy to reliably sample. They are rapidly reproducing organisms with wide dispersal abilities (Cowen and Sponaugle, 2009; Marcot, 1976; McManus and Woodson, 2012) and their short generation times (day to months) allow population responses to intra-seasonal environmental changes. While integrating short-term, daily to weekly, events. Second, while ecosystem productivity seems to be under the control of the physical dynamics (Bi et al., 2011b; Gao et al., 2021; Heath and Lough, 2007; Helaouët and Beaugrand, 2007; Keister et al., 2011; Roemmich and McGowan, 1995), many planktonic species are characteristic of specific water masses (Bi et al., 2011a; Burckle, 1998; Liu et al., 2015; McGowan and Walker, 1979; Reid et al., 1978). Third, many studies have demonstrated that changes in plankton are considered among the earliest and most sensitive ecosystem responses to both anthropogenic pressure (Attayde and Bozelli, 1998; Bedford et al., 2018; Schindler, 1998; Serranito et al., 2016) and global environmental/climate change (Beaugrand et al., 2015; Bi et al., 2014; Doney and Sailley, 2013; Winder and Sommer, 2012). Finally, zooplankton are rarely commercially exploited and support many predators; they are therefore fishery-independent and less affected by the unknown and confounding factors that complicate the interpretation of indicators.

Developing plankton indicators that target coastal and estuarine systems remains a challenging task due to the inherent stochasticity of plankton dynamics and the sensitivity of indicators to climate-driven changes (Bedford et al., 2020). In such systems, plankton are influenced by processes at different temporal scales, including daily tidal cycles, diurnal cycles, spring-neap cycles, seasonal cycles, episodic events like flooding or changes in circulation patterns, as well as complex biological processes.

To parse the impacts of the different processes and to reduce the uncertainties in plankton indicators, there is a definite and clear need for continuous intensive monitoring programs. Traditional sampling approaches, such as nets, can be expensive and labor-intensive and it is time consuming to process plankton samples under the microscope; in addition, the time lag between sampling and data analysis/interpretation makes it difficult to provide plankton indicators to policy makers in a timely manner (Benfield et al., 2007).

In the past few decades, the development of imaging systems in combination with the rise of artificial intelligence has given scientists more options to measure zooplankton in a faster, convenient, and more comprehensive way. In addition to their non-invasive collection of data, imaging systems can autonomously acquire images in real-time for organisms from single-celled phytoplankton, microzooplankton, to multiple-celled mesozooplankton, larval fish and jellyfish: Imaging Flow Cytobot (Olson and Sosik, 2007), Video Plankton Recorder (Davis et al., 1992), Underwater Video Profiler (Picheral et al., 2010), In Situ Ichthyoplankton Imaging System (Cowen and Guigand, 2008), GUARD1

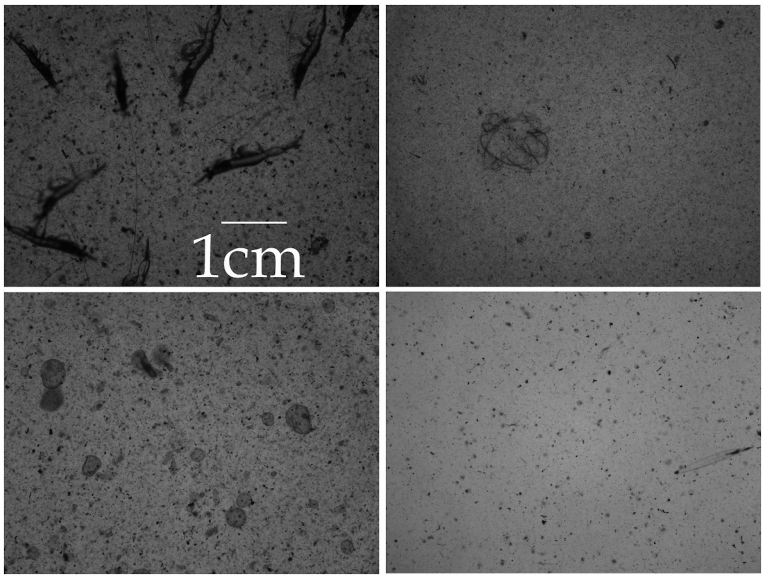

Fig. 2. Example images collected in the study site, showing mysid shrimps (upper left), jellyfish (upper right), colonies of *Phaeocystis* (lower left), and chaetognaths and *Noctiluca* (lower right). Note the dense particles in the images, which highlight the challenges of imaging plankton under the suboptimal conditions at the study site.

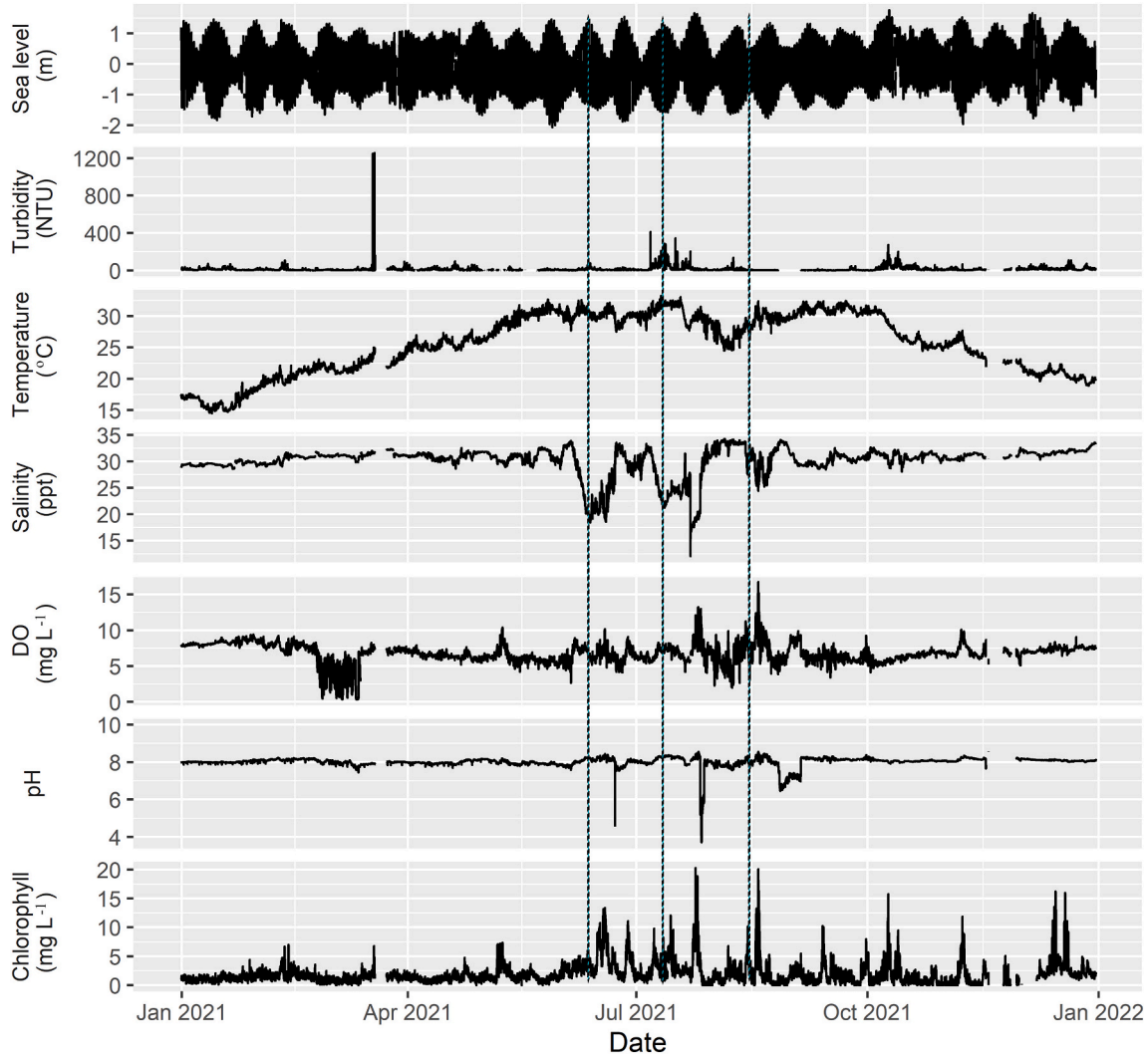

Fig. 3. Times series of hourly environmental variables. The three dashed vertical lines indicate typhoon events in June – August 2021.

Table 1
Monthly means and standard deviations of environmental variables.

	Sea level(m)		Turbidity (NTU)		Temperature (°C)		Salinity (ppt)		Dissolve oxygen (mg L^{-1})		pH		Chlorophyll (mg L^{-1})	
Month	Mean	SD	Mean	SD	Mean	SD	Mean	SD	Mean	SD	Mean	SD	Mean	SD
1	−0.13	0.66	12.81	10.65	16.48	1.13	29.48	0.35	8.29	0.36	8.01	0.04	1.21	0.48
2	−0.17	0.62	8.47	9.92	20.63	1.06	30.55	0.72	7.28	1.52	8.12	0.07	1.71	0.89
3	−0.16	0.64	15.78	85.86	22.32	1.04	31.23	0.50	5.51	2.27	7.94	0.10	1.32	0.67
4	−0.09	0.64	13.91	14.29	25.60	0.70	30.99	0.61	6.47	0.42	7.98	0.08	1.25	0.59
5	−0.28	0.72	5.76	5.46	29.90	1.59	31.14	0.89	5.89	0.63	7.93	0.08	1.50	1.02
6	−0.26	0.65	9.20	9.04	30.18	0.88	27.10	4.79	6.66	1.04	8.01	0.24	3.94	2.48
7	−0.17	0.63	32.84	53.75	30.42	1.36	26.32	4.37	7.02	1.36	7.99	0.61	2.92	2.79
8	−0.28	0.64	7.07	10.66	28.23	1.82	31.41	2.57	7.07	2.29	8.00	0.21	2.42	2.86
9	−0.14	0.63	3.97	5.75	31.17	0.58	30.13	0.84	6.28	0.76	8.17	0.07	1.65	1.60
10	0.12	0.62	27.14	31.92	27.31	2.18	30.97	0.80	6.26	0.62	8.06	0.05	1.46	1.70
11	−0.04	0.64	9.50	7.79	24.87	1.30	30.94	0.46	7.08	0.84	8.15	0.08	1.42	1.93
12	−0.01	0.59	20.73	16.75	20.49	0.76	31.96	0.66	7.44	0.30	8.08	0.03	2.86	1.83

system (Corgnati et al., 2016), PlanktonScope (Song et al., 2020), Scripps Plankton Camera system (Campbell et al., 2020; Merz et al., 2021; Orenstein et al., 2020) are among the commonly used in situ imaging systems. The advanced deep learning systems such as convolutional neural networks (CNNs) have dramatically sped up our ability to identify and enumerate plankton images with high accuracy (Cheng et al., 2019; Irisson et al., 2022; Luo et al., 2018). Most plankton imaging systems include the digital storage of individual photographs and measurements, making data verification and exchange easier. Deploying plankton imaging systems in productive coastal and estuarine systems remains challenging (Bi et al., 2012a; Song et al., 2020), however, because of the sub-optimal imaging conditions caused by high turbidity and dynamic environment, and the difficulty of processing noisy images (Bi et al., 2015; Song et al., 2022).

The objectives of our study are to: (1) develop plankton indicators for the Guangdong coastal water using data collected by PlanktonScope, and in particular to provide early warning of swarms of mysids and jellyfish which have the potential to clog cooling water intakes, (2) identify the temporal characteristics of plankton indicators by taking advantage of the high-frequency sampling provided by the PlanktonScope, and (3) quantify the impacts of different physical processes across a range of temporal scales on plankton density.

2. Sampling and data analysis

2.1. Sampling site and hydrography

The Guangdong province is located in the southernmost part of China. Its coastal waters are heavily affected by dense urban populations and industrial wastewater. As a subtropical region, the large-scale circulation pattern is mostly driven by the East Asian Monsoon or Meiyu (Bakun, 1973; Ding and Chan, 2005; Tung et al., 2020). Three tropical cyclones landfalls in coastal areas of Guangdong occur on average each year (Knapp et al., 2018). The eastern part of Guangdong coast is affected by summer upwelling, the Pearl River plume, the westward coastal current, and northeastward current in the open ocean (Chen et al., 2017; Gan et al., 2014; Guan, 1978). It is an ideal location to examine the interactions between plankton and their biotic and abiotic environments and changes over time. In this region, common, large, blooming plankton include *Lyngby* sp., *Phaeocystis* sp., and *Noctiluca* sp. (Gui et al., 2020). The dominant zooplankton groups are copepods, jellyfish, chaetognaths, appendicularians, and meroplanktonic larvae (Gong et al., 2019).

The study site was established in a small man-made harbor since January 1, 2021, in front of an industrial cooling water intake off Yangjiang, the central Guangdong coast (21.72°N and 111.96°E, Fig. 1). The study area is influenced by east Asia monsoons and characterized by a wet summer in May – September and a dry winter in October – April. Prevailing winds are northerly monsoon during winter and southerly during summer (Xie et al., 2015; Zhou et al., 2008). The local currents include a westward alongshore current along the coast and a northeastward current in the open sea (Guan, 1978). The most prevalent tidal pattern is semi-diurnal with two high and two low tides per tidal day and the average difference between high tide and low tide is 1.12–1.48 m (Zhou et al., 2008).

3. Methods

PlanktonScope (Liu, 2021; Song et al., 2020) and its predecessor ZOOplankton VISualization system (ZOOVIS, Bi et al., 2012a; Trevorrow et al., 2005) were designed as open area, shadowgraph imaging system to maximize imaging capability in turbid coastal and estuarine waters. PlanktonScope is equipped with a specially designed illumination system which uses relatively long wavelength red light at 640 nm to reduce attenuation and minimize the disturbance of organisms (Davis et al., 1992). The illumination system operates in strobe mode, which produces more light for a limited amount of time and achieves higher intensities than the nominal output values. The strobe mode is designed to overcome fast attenuation due to high particulate concentration in turbid coastal waters and provide adequate light to image fast-moving objects. At the same time, the strobe mode helps preserve the life span of the illumination system and reduces power consumption. Most importantly, the illumination system synchronizes the acquisition time of the camera and lighting, and reduces to exposure time to 2 μs, which eliminates the influence of ambient light and overcomes motion blur in coastal and estuarine environments caused by ocean currents often reaching 1 m s^{-1} (Cresswell, 2000).

The PlanktonScope system includes two pressure housings: an illumination pod which includes the illumination system and a battery pack, and a camera pod which includes camera, lens, computer board and storage. PlanktonScope is equipped with a high-density digital camera with a complementary metal oxide semiconductor (CMOS) image sensor with a field of view 57 mm × 43 mm. A special designed reflecting camera lens extends the depth of field to 105 mm. The sample volume for each image is ~256 ml. The relatively large field view and the 20 μm pixel resolution allows the system to image plankton as small as ~50–100 μm. The distance between the camera pod and illumination pods is 16 cm.

The water depth at the sampling site in the channel for cooling water intake was ~8–9 m depending on tidal cycle and the current persistently moved landward with a relatively stable unidirectional landward velocity > 1 m s^{-1} (Fig. 1). The persistent high speed water intake essentially acted as a coastal water trap.

PlanktonScope was deployed from January 1 to December 31, 2021 at ~3 m within the bottom and collected images at 0.05 Hz (3 images per minute). Maintenance and service were performed every two weeks in June – October and every three weeks in other months to clean and prevent biofouling. In total, ~1.3 million images were collected and

Table 2
Monthly means and standard errors of nine plankton groups observed by PlanktonScope.

	Phaeocystis		*Lyngbya*		*Noctiluca*		Jellyfish		Appendicularia		Copepod		Echinodermata larvae		Chaetognatha		Shrimp	
Month	Mean	Std	Mean	Std	Mean	Std	Mean	Std	Mean	Std	Mean	Std	Mean	Std	Mean	Std	Mean	Std
1	5.17	12.99	2063.55	8259.91	2837.52	6200.48	7.73	17.07	13.06	45.13	80.02	191.27	68.12	127.50	14.94	23.66	16.98	29.28
2	12.20	18.76	214.36	681.34	9850.15	17,515.69	14.29	23.97	2.03	8.34	5.90	26.09	385.52	1042.36	14.56	24.13	10.86	23.36
3	0.00	0.00	8859.50	59,866.94	8124.78	15,959.23	7.30	19.23	72.65	134.24	32.26	82.51	1959.34	3792.93	33.31	52.25	28.74	83.70
4	0.00	0.00	40.09	807.20	301.06	986.91	16.09	30.09	22.92	61.43	8.08	30.08	157.36	965.51	56.55	94.75	23.56	75.48
5	0.00	0.00	132.68	777.35	86.29	288.60	22.85	65.67	128.74	205.11	31.90	69.71	982.24	3054.87	94.31	125.21	22.20	29.72
6	0.00	0.00	58.89	1341.77	20.25	176.97	5.35	27.91	25.51	62.17	48.17	255.37	14.05	52.43	15.88	34.88	12.66	38.96
7	126.64	852.25	19.69	219.99	2.76	14.61	3.54	13.01	17.25	94.68	12.57	39.05	4.61	22.41	3.25	10.39	6.61	17.25
8	132.08	265.73	65.12	644.41	198.41	988.77	24.53	57.08	16.08	48.40	20.18	64.73	281.61	1072.82	55.11	113.02	15.41	25.53
9	0.00	0.00	93.87	1287.38	4.95	14.82	74.88	90.89	34.75	66.73	7.92	29.96	49.26	184.26	79.51	93.47	75.63	96.96
10	255.98	745.94	7.06	38.75	0.11	1.36	4.93	22.27	2.69	13.68	14.20	39.54	2.31	15.60	9.18	19.51	2.44	10.99
11	5082.34	7179.55	167.08	1237.61	0.00	0.00	35.00	59.14	1.88	8.05	156.69	273.06	105.65	378.58	38.66	45.27	5.79	16.55
12	170.97	490.39	69.65	492.74	116.26	451.82	4.59	10.74	4.53	19.56	50.94	90.53	11.74	82.08	28.49	57.86	2.20	8.09

analyzed. Here, we focused on copepods, appendicularians, chaetognaths, jellyfish, mysids, *Noctiluca* and Phaeocystis, which account for >90% counts. The fast landward flow speed and relatively low imaging frequency ensured no duplicate images of the same individual organism. Plankton count data were binned hourly for analysis.

Environmental data including water level, temperature, salinity, pH, optical dissolved oxygen (ODO) and chlorophyll *a* from fluorescence were measured every 30 s by a buoy at the same location. Environmental data were binned hourly.

3.1. Image processing

PlanktonScope is equipped with an end-to-end integrated image processing system begins with a scene classifier to capture large within-image variation, followed by the pretrained scene-specific regional convolutional neural network (Mask R-CNN) models to separate target objects into different taxonomic groups (Bi et al., 2022). This new end-to-end approach overcomes the issues of separating potential targets from noisy low contrast backgrounds and large variations in image contents (Fig. 2) and is capable of processing 10–25 images per minute depending upon image content. This framework can enumerate and store segmented images for a total of 19 plankton groups (Bi et al., 2022). The system was deployed to process in situ images collected by PlanktonScope and to provide near real time plankton density, specifically mysid shrimp data because mysid swarms could clog cooling water intake. In this study, we reclassified the segmented targets using another automated procedure based on residual neural network with an accuracy ~92% (Cheng et al., 2019; Cheng et al., 2020; Jiao et al., 2022; Song et al., 2022).

3.2. Data analysis

By nature, time series of plankton measure plankton status over time. Each observation reflects the impacts of multiple interacting processes at a given time and our ability to distinguish the impacts from different processes is often determined by sampling frequency. However, by examining the periodic signals in environmental factors and selected plankton indicators, we can identify the prevailing temporal characteristics in plankton indicators and environmental factors, and match them in the frequency domain.

We applied wavelet-transform-based technique on each hourly binned environmental factor and biological variable to analyze the presence of different frequencies in each variable (Torrence and Compo, 1998). A Morlet wavelet was selected as a basis function, which represents an optimal balance between time and frequency localization for features in wavelet spectra. Prior to analysis, we first filled the data gaps in time series, using (1) linear interpolation for data gaps of <24-h and (2) neighboring daily means for the few extensive gaps (3–5) that lasted a few days. By doing so, we did not contaminate the spectra results derived from valid observations. For visualization, a log transformation was applied to biological observations. Biological activities being highly seasonal, results from wavelet analysis provide useful information to identify bloom periods and can guide further investigation for the corresponding environmental process. The hourly data of one-year measurements can statistically resolve the variability on time scales from hours to season.

To examine the impact of diurnal cycle, we created a second variable to indicate whether observations occurred in daytime or nighttime. For the analysis of the seasonal monsoons, i.e., dry winters and wet summers, May – October were considered as wet summer season and the other months as dry season (Kim et al., 2013). To quantify the impacts of physical processes on plankton abundance, we identified the daily peaks for each plankton group. Given the large number of zeros and to avoid potential white noise interference, we eliminated peaks with density less than the mean abundance. Based on the peaks we identified, a new binary variable was created to indicate the occurrence of daily peak. For

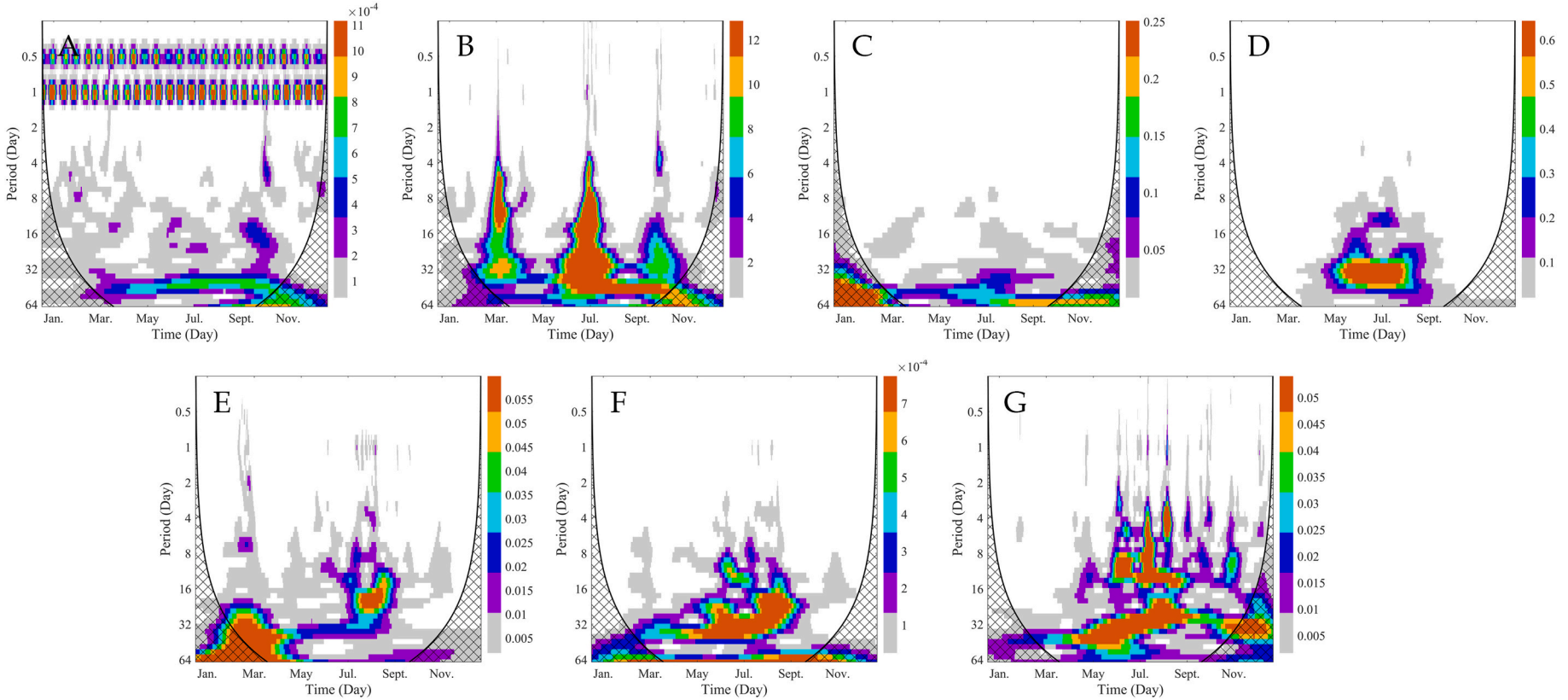

Fig. 4. Power spectra of environmental factors: A, sea level; B, turbidity; C, temperature; D, salinity; E, dissolved oxygen (DO); F, pH; and G, chlorophyll *a*. Note that cross-hatched regions on either end indicate the "cone of influence," where edge effects become important and therefore the derived frequencies are not reliable.

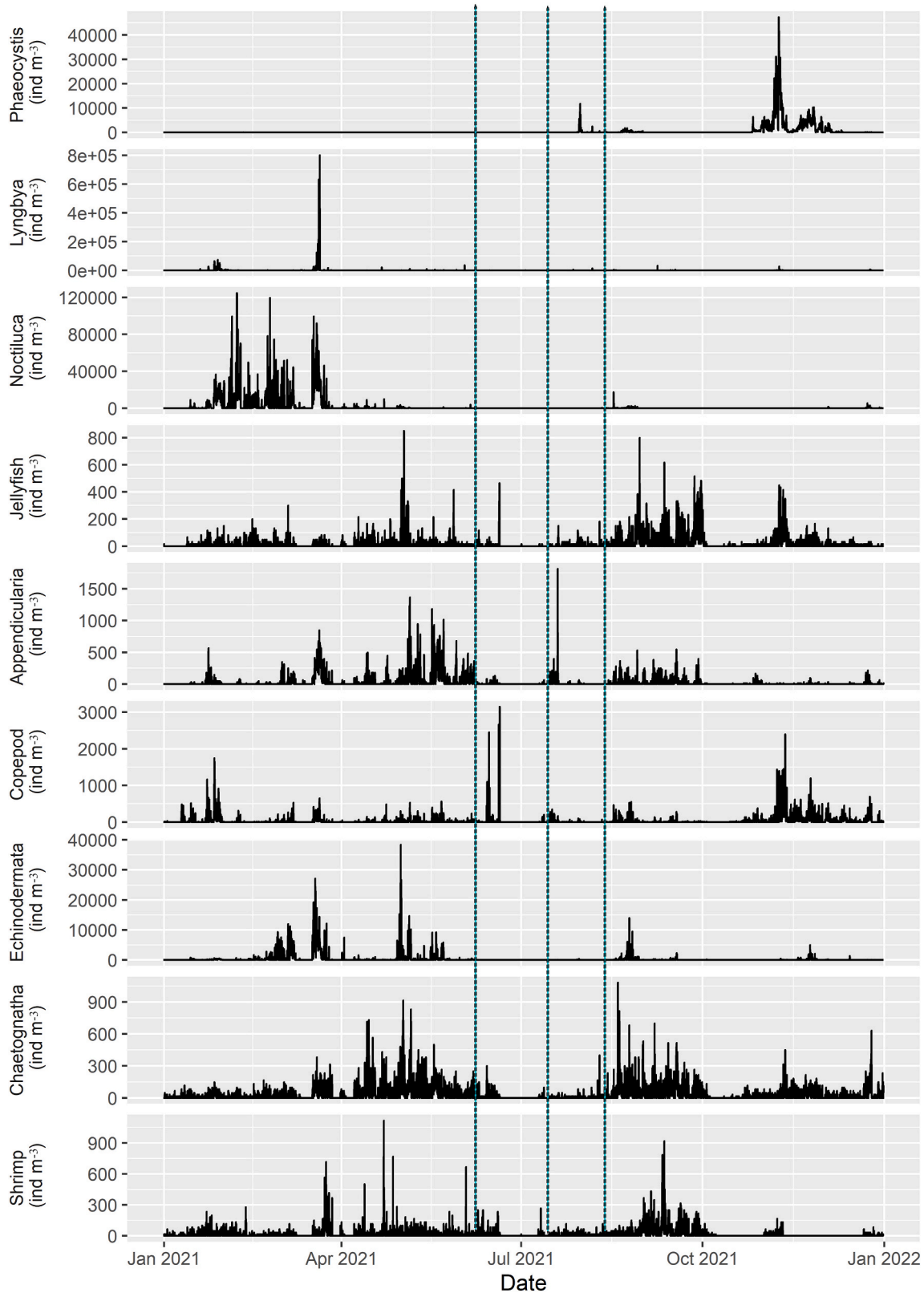

Fig. 5. Time series of the nine dominant plankton groups observed by PlanktonScope in 2021. The three vertical dashed lines indicate three typhoon events between June and August 2021.

each plankton group, a logistic regression model was constructed to examine the occurrence of peaks in relation to diurnal cycles, tides, and seasonal monsoon patterns (Bi et al., 2008; Kleinbaum et al., 2002).

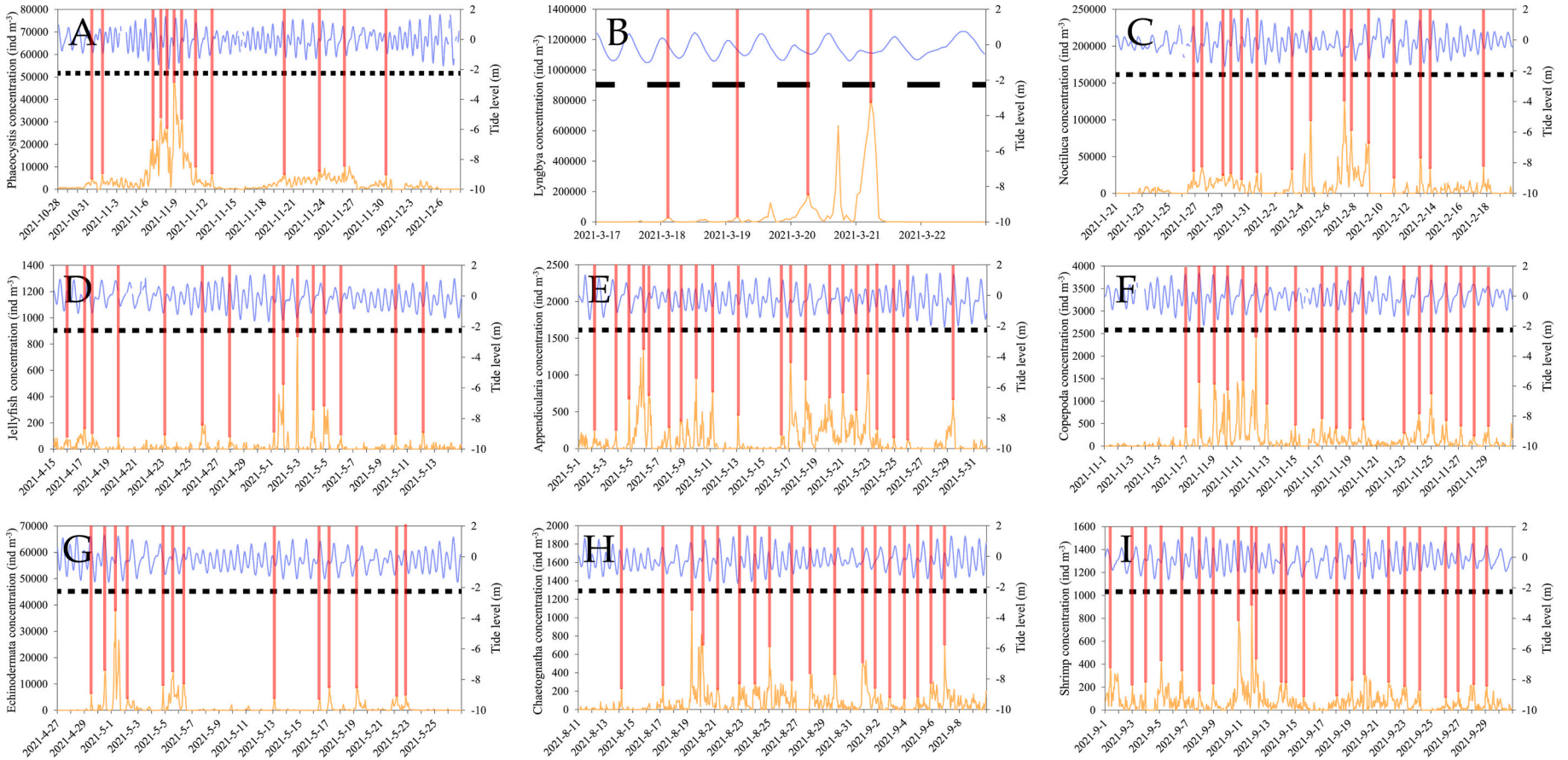

Fig. 6. Example of relationship between tidal and diurnal cycles and plankton abundance. Note that different taxa peaked at different times and the selected period of high abundance varied for different groups. Light blue lines indicate tidal cycles, black dashed lines indicate diurnal cycles with black for nighttime and white for daytime, and orange lines indicate plankton abundances. Red vertical lines indicate daily peaks. A *Phaeocystis*, B *Lyngbya*, C *Noctiluca*, D jellyfish, E appendicularians, F copepods, G echinoderm larvae, H chaetognaths, I shrimps. (For interpretation of the references to colour in this figure legend, the reader is referred to the web version of this article.)

Table 3
Results of logistic regression models. Bold font indicates statistical significance.

		Estimate	Std Error	z value	P (>|z|)			Estimate	Std Error	z value	P (>|z|)
	(Intercept)	−4.68	0.33	−14.22	**<0.01**		(Intercept)	−5.57	0.31	−17.71	**<0.01**
	Diurnal	0.21	0.38	0.55	0.58		Diurnal	1.49	0.28	5.31	**<0.01**
Phaeocystis	Tide	−0.04	0.49	−0.08	0.94	Copepod	Tide	−0.11	0.42	−0.25	0.8
	Monsoon	−2.15	0.43	−5.05	**<0.01**		Monsoon	−0.03	0.23	0.14	0.88
	Diurnal*Tide	−0.01	0.62	−0.01	0.99		Diurnal*Tide	0.84	0.46	1.85	0.06
	(Intercept)	−6.81	0.58	−11.76	**<0.01**		(Intercept)	−6.45	0.47	−13.73	**<0.01**
	Diurnal	0.07	0.38	0.2	0.84		Diurnal	0.78	0.29	2.71	**<0.01**
Lyngbya	Tide	1.04	0.4	2.61	**<0.01**	Echinoderm larvae	Tide	0.26	0.39	0.67	0.51
	Monsoon	1.41	0.55	2.57	**0.01**		Monsoon	1.22	0.44	2.77	**<0.01**
	Diurnal*Tide	0.42	0.54	0.79	0.43		Diurnal*Tide	−0.06	0.46	−0.13	0.89
	(Intercept)	7.56	0.75	−10.03	**<0.01**		(Intercept)	−5.01	0.25	−19.89	**<0.01**
	Diurnal	0.62	0.31	1.98	**0.05**		Diurnal	0.95	0.2	4.64	**<0.01**
Noctiluca	Tide	0.33	0.41	0.8	0.42	Chaetognatha	Tide	0.37	0.29	1.28	0.2
	Monsoon	2.25	0.73	3.08	**<0.01**		Monsoon	0.26	0.22	1.2	0.23
	Diurnal*Tide	0.31	0.5	0.64	0.52		Diurnal*Tide	0.01	0.33	0.02	0.98
	(Intercept)	−5.28	0.27	−19.45	**<0.01**		(Intercept)	−5.66	0.32	17.87	**<0.01**
	Diurnal	1.07	0.21	5.01	**<0.01**		Diurnal	0.82	0.2	4.03	**<0.01**
Jellyfish	Tide	0.44	0.3	1.47	0.14	Shrimp	Tide	0.52	0.27	1.9	0.06
	Monsoon	0.48	0.23	2.01	**0.04**		Monsoon	1.1	0.29	3.77	**<0.01**
	Diurnal*Tide	−0.06	0.34	−0.17	0.87		Diurnal*Tide	−0.18	0.32	−0.56	0.56
	(Intercept)	−5.84	0.37	−15.92	**<0.01**						
	Diurnal	0.59	0.23	2.59	**<0.01**						
Appendicularia	Tide	0.78	0.29	2.71	**<0.01**						
	Monsoon	1.12	0.35	3.26	**<0.01**						
	Diurnal*Tide	−0.4	0.35	−1.13	0.26						

4. Results

4.1. Environmental conditions

Sea level data showed strong periodic signals ranging from −2.07–1.77 m with the maximum value occurring on October 10 and the minimum value occurring on May 28 (Fig. 3). Monthly mean sea level was higher in dry winter and lower in wet summer (Table 1). Turbidity was high with a mean of 14.73 ± 0.38 NTU (mean ± standard error) which underscored the challenges of imaging plankton at the study site (Fig. 3). Monthly mean turbidity showed large variations and no clear seasonal pattern (Table 1). Surface water temperature ranged from 14.47 to 33.25 °C with the minimum temperature on January 13 and maximum on July 11 (Fig. 3). Monthly mean temperature showed strong seasonal pattern (Table 1), while salinity had high variability (Fig. 3 and Table 1) clearly dominated by the typhoons during summer monsoon. It ranged from 12.0 to 34.30, with a mean 30.15 ± 0.03, and lowest values during and after the typhoon events. Dissolved oxygen and pH did not show clear seasonality, but were affected by typhoon events (Fig. 3 and Table 2). Fluorescence-derived chlorophyll-*a* concentration showed large fluctuation over time (Fig. 3) and ranged from 0 to 20.32 mg L^{-1} with a mean of 1.98 ± 0.02 mg L^{-1}. Monthly mean chlorophyll *a*ppeared to be higher during summer monsoon in June – August and in December (Table 1).

4.2. Power spectra of environmental variables

On the frequency domain, sea level data contained evident tidal periodicity and the corresponding peaks at the semidiurnal and diurnal frequencies were persistent throughout the year (Fig. 4A). The water pumps for industrial cooling facilities induced intense mixing in the small harbor and basically homogenized the temperature and salinity in the intake channel (Fig. 4C–D). Short-term variability due to advection of tidal current or heat fluxes over day/night cycle was mostly masked. The impacts of tides were discernible for turbidity, dissolved oxygen, pH, and chlorophyll *a* (Fig. 4B, E–G).

Weather events such as typhoons and storms occurred three times in 2021 and each event lasted a few days. They were often accompanied by intense winds and significantly increased/decreased precipitations and heat fluxes. They consequently affected the local environment, such as sea level, temperature, salinity, and turbidity. For instance, the high spectra values at the time scales of day-weeks occurred in the sea level data in June – September. Their fingerprints on oxygen, turbidity and chlorophyll *a* were only detectable in June – September, which was consistent with the active periods of those environmental factors.

Atmospheric processes, such as monsoon and Meiyu front, can remain over southern China for months and they often lead to changes in wind direction and intensity, persistent rainfalls and increased river discharge, which in turn tend to reduce salinity in the study region. The modified wind-driven currents also play an important role in the decrease of the nearshore salinity by transporting fresher river plumes along the southeast coast of China. Such processes are confirmed by the widespread peaks in the spectra of temperature, salinity, oxygen, pH and turbidity at the time scales of months (~30 days).

4.3. Seasonal dynamics of plankton abundance

With PlanktonScope, we identified nine dominant plankton groups over the full year of sampling. Three large phytoplankton groups sampled by PlanktonScope showed strong seasonal variations, with colonies of *Phaeocystis* blooming post wet monsoon season and *Noctiluca* and the line-shaped algae *Lyngbya* blooming pre wet monsoon season (Figs. 2, 5 and Table 2). The peak abundances of *Phaeocystis*, *Lyngbya* and *Noctiluca*, were much higher than their mean abundances, 4.73 × 10^4, 8.02 × 10^5 ind. m^{-3} and 2.15 × 10^4, respectively versus 477.34 ± 27.36, 998.73 ± 190.07, and 1747.79 ± 82.24 ind. m^{-3}, respectively. However, the peak bloom duration of *Phaeocystis* and *Lyngbya* appeared to be short-lived, ~ one – two weeks, while *Noctiluca* blooms tended to be relatively long, ~ two weeks – one month.

Jellyfish, appendicularians, copepods, echinoderm larvae, chaetognaths and shrimps also showed strong seasonal variation with relatively higher abundance during the summer monsoon than in winter (Fig. 5 and Table 2). The variability of these zooplankton groups was generally lower than that of the large phytoplankton groups, except for echinoderm larvae which had a coefficient of variation (CV) of 4.78. The CVs for other zooplankton groups ranged from 2.01 to 3.49 and that of the three large phytoplankton groups ranged from 4.41 to 17.81. The abundance of echinoderm larvae was the highest in April and June, 3.84 × 10^4 ind. m^{-3}. On average, the abundance of echinoderm larvae accounted for 23% of total zooplankton counts, and chaetognaths,

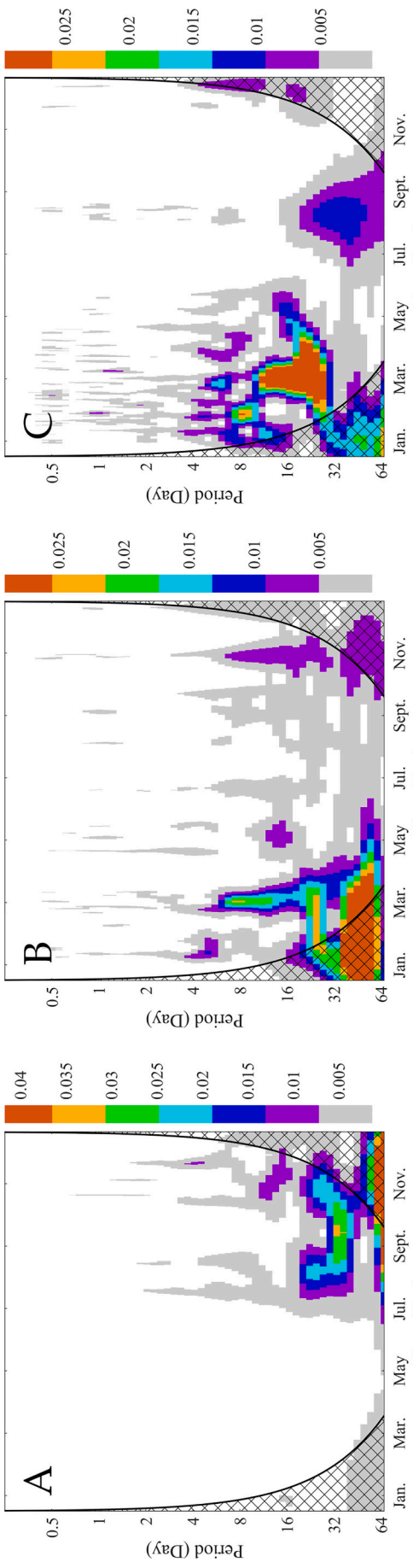

Fig. 7. Power spectra of large phytoplankton abundance time series. A *Phaeocystis*, B *Lyngbya*, and C *Noctiluca*. Note that cross-hatched regions on either end indicate the "cone of influence," where edge effects become important and therefore the derived frequencies are not reliable.

shrimps, copepods, jellyfish and appendicularians accounted for 22%, 17%, 16%, 13%, and 8% of the total abundance, respectively. While the three typhoon events which occurred in June – September 2021 appeared to have strong negative impacts on zooplankton abundance (Fig. 5), copepod and appendicularians peaked during or after the first (June) and the second (July) typhoon event, respectively. The exact impacts of typhoon events on zooplankton and the underlying mechanisms, e.g., through high mortality or changes in water masses, remain unclear.

4.4. Power spectra of plankton data

High-frequency data are ideal to examine the fine-scale temporal variation of plankton. For example, the high-frequency data during the selected blooming periods for different plankton groups showed that many plankton groups showed a clear diurnal cycle with daily peaks occurring in nighttime, while tidal impacts were less obvious, except that copepod daily peaks mostly occurred around high tide (Fig. 6). Results from logistic regression based on full-year data further showed that the daily peaks of six zooplankton groups showed clear diurnal cycles with peaks during nighttime. No clear diurnal patterns were detected for the daily peaks of phytoplankton groups (Table 3). Tidal impacts were only significant for *Lyngbya* and appendicularia. The impacts of monsoon season were significant for all the plankton groups.

On the frequency domain, peaks in energy with semidiurnal and diurnal frequency were relatively weak in the power spectrum, suggesting that these variations contribute less to the total variability than the seasonal and episodic components (Figs. 7 and 8). Their short-term variability, due to advection of tidal currents or heat fluxes over day/night cycles, were mostly masked by stronger signals at biweekly – bimonthly periods. These biweekly – monthly frequencies were consistent with plankton reproduction and growth cycles: weekly – biweekly periods for phytoplankton groups (Fig. 7) and biweekly – monthly for zooplankton groups (Fig. 8).

Weather events such as typhoons and storms usually lasted a few days, and they showed strong negative impacts on zooplankton groups, as indicated by the high spectra values at the time scales of days-weeks in the sea level data. The impacts of seasonal patterns such as monsoon and Meiyu front were evident at quarterly – semi-annual scales (Figs. 7 and 8).

5. Discussion and conclusions

Our study illustrates that near real-time high-frequency plankton data are useful to examine population dynamics, potential trophic interactions, process studies, environmental associations, and size structure at different temporal scales. By sampling different species simultaneously, imaging systems provide a robust, holistic view of the dynamics of pelagic ecosystems, and therefore insights on potential trophic interactions among different groups. For example, the positive correlations we found between *Lyngbya* and other plankton groups indicate a synchronous presence that suggests that the common algae may be a food source for several zooplankton groups (Fig. 9). The positive relationships between echinoderm larval density and several other plankton groups suggest potential predator-prey interactions. Negative relationships between the density of *Phaeocystis* and most other plankton groups suggest potential impacts of *Phaeocystis* blooms (Breton et al., 2021).

5.1. Advantages of imaging systems for plankton monitoring

Plankton imaging systems are increasingly used in ecosystem monitoring (Orenstein et al., 2020; Romagnan et al., 2016; Rutten et al., 2005; Song et al., 2022). As we revealed in our study, they offer several advantages over traditional sampling and can provide useful information for ecosystem assessment and for developing new indicators or

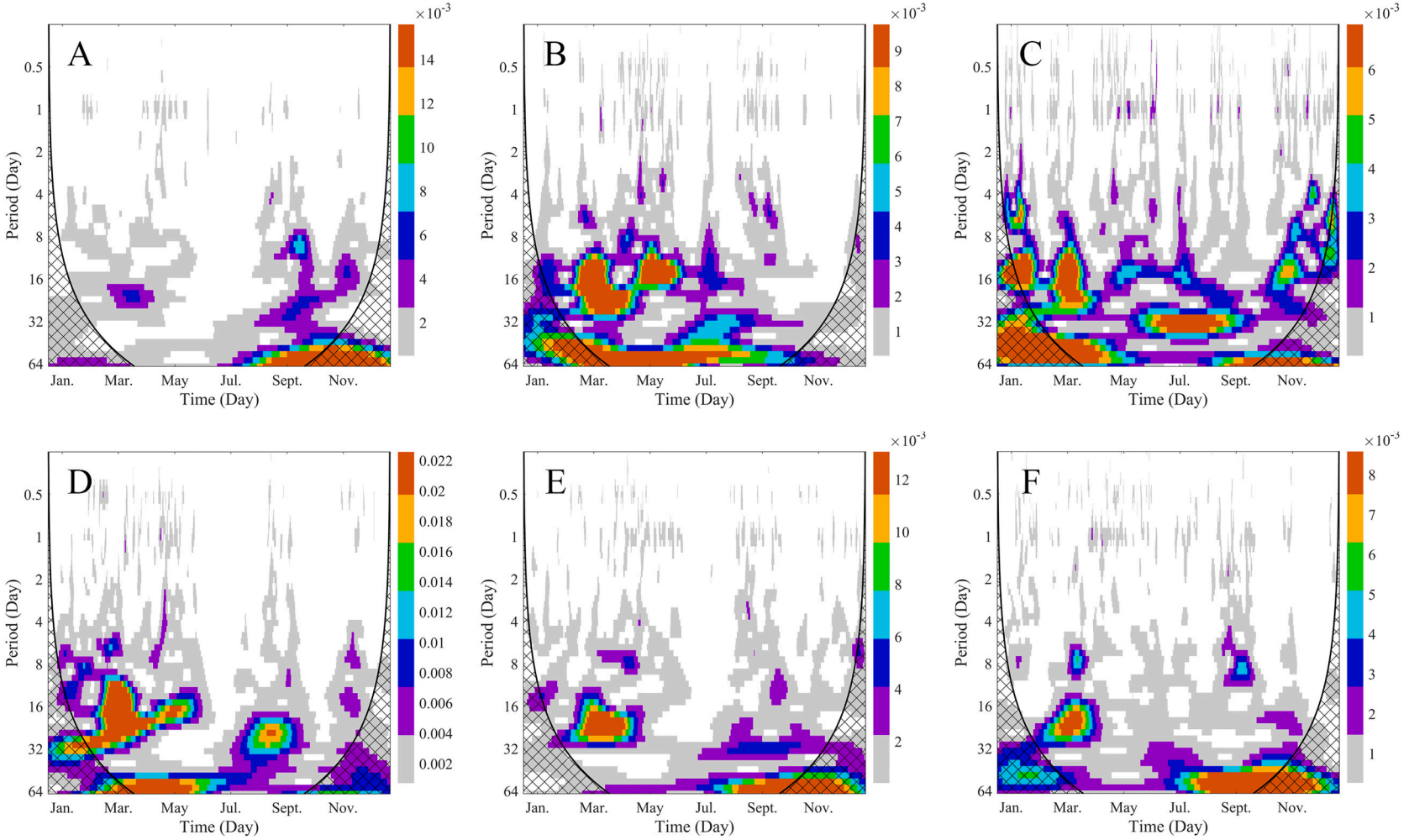

Fig. 8. Power spectra of zooplankton abundance time series. A jellyfish, B appendicularians, C copepods, D echinoderm larvae, E chaetognaths, F shrimps. Note that cross-hatched regions on either end indicate the "cone of influence," where edge effects become important and therefore the derived frequencies are not reliable.

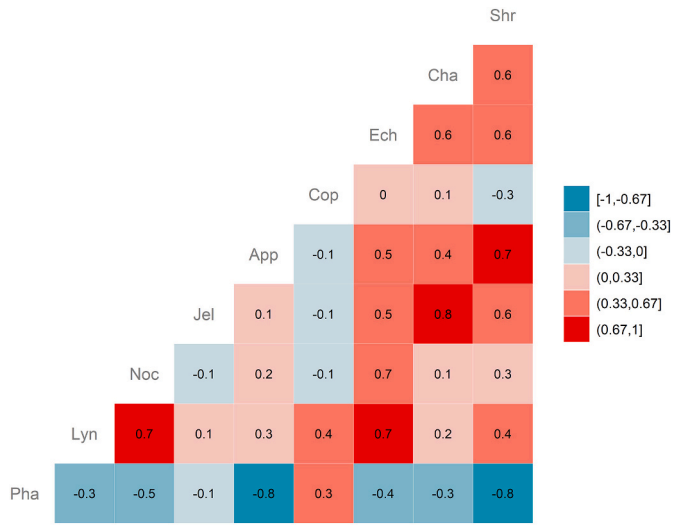

Fig. 9. Spearman correlation among different plankton groups. Abbreviations: Pha for *Phaeocystis*, Lyn for *Lyngbya*, Noc for *Noctiluca*, Jel for jellyfish, App for appendicularian, Cop for copepod, Ech for echinoderm larvae, Cha for chaetognath, and Shr for shrimp.

refining existing ones: (1) they produce simultaneous measurements on a suite of plankton indicators which can characterize the status of the pelagic ecosystem effectively; (2) in combination with artificial intelligence, they provide real-time or near real-time information as opposed to waiting for months or years before data from net samples become available; (3) they enable high-frequency and high resolution sampling in both time and space, and thus improve the accuracy of the indicators and increase our ability to identify the underlying mechanisms for the observed dynamics; (4) they overcome the issue of filtration efficiency with different mesh size and towing speed (Hosia et al., 2017) and provide new means to sample highly aggregated species, such as krill and mysids, and rarer and more fragile species, such as gelatinous zooplankton, which are difficult to sample using traditional sampling gears (Corgnati et al., 2016); (5) imaging systems in combination with machine learning methods can measure body size along with other morphological traits such as transparency and luminescence (Orenstein et al., 2022), which enable development of indicators based on relative size composition and other morphological traits; (6) imaging systems can capture zooplankton in their natural orientations and typical behaviors (Möller et al., 2012; Möller et al., 2020), which may allow new functional grouping and corresponding indicators; (7) imaging systems can capture early life stages of economically important species, such as shrimps and crabs, to design recruitment indices; and (8) the image system high-frequency sampling can correctly identify the blooms of fast-reproducing organisms such as phytoplankton.

5.2. *Understanding high-frequency time series of plankton data*

Despite the importance and increasing availability of high-frequency plankton data, there is a clear lack of tools -or specific guidelines- for analyzing such data. High-frequency plankton imaging systems are ideal to study processes at different scales. For example, most phytoplankton groups show strong and rapid temporal dynamics (shown clearly in our data) and relatively short life spans, and traditional monthly sampling may miss the blooms and misplace the phytoplankton frequency distribution, leading to difficulties in accurately assessing the species phenology, its changes over time, and the influence of environmental conditions (Wu et al., 2016). On the other hand, high-frequency imaging systems can monitor rapid changes and provide the correct information for the phenology of the groups at the basis of the marine food chain.

Several reviews summarized physical and biological processes cross different time and spatial scales (Daly and Smith, 1993; Dickey et al., 2001) and there is little doubt that plankton dynamics manifest physical and biological processes at different scales. But the challenge is that different plankton manifest impacts differently. Several mechanisms have been proposed to explain how planktonic organisms maintain their populations in estuaries and coastal waters and most are related to the nonuniform characteristics of ocean currents, including temporal varying speed and direction and different patterns in horizontal and vertical space (Jeannette, 2002; Pineda, 1991; Show, 1980). The continuum approach allows a comparison as a function of temporal and spatial scales, demonstrating overlap and interlace (Fig. 10).

Tidal and ocean currents can cause significant dispersive and advective losses, or accumulation of planktonic organisms. However, populations typically have their highest density over regions with

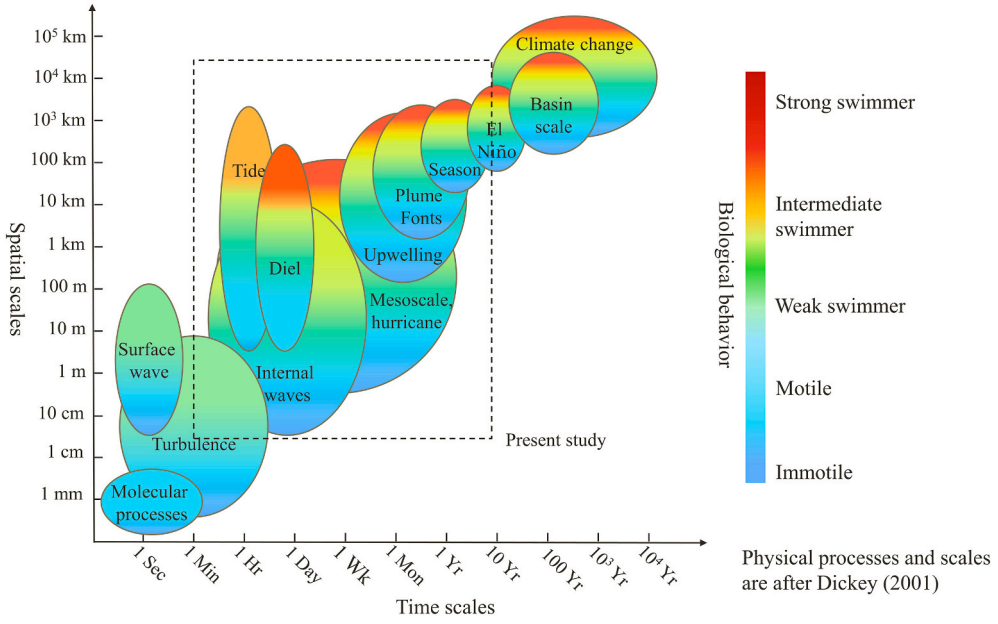

Fig. 10. Spatial and temporal scales of physical processes in the study area and differential impacts on planktonic organisms based on their motility (After Dickey et al., 2001).

certain environmental conditions, e.g. salinity, implying a mechanism for retention, concentration or survival (Clancy and Cobb, 1997; Cross et al., 2015; Mackas et al., 1985).

Unique coastline configuration and bathymetry can lead to asymmetric tidal currents in flood and ebb tidal phases. Organisms residing in a flood tidal current might experience much weaker flow during ebb tides. Consequently, a large fraction of the abundance is retained over a tidal cycle. In addition, bottom friction can reduce the ocean current near the bottom. Organisms can avoid washout via behaviors that keep them near seafloor where they are less likely to be entrained in unfavorable flows. This requires stronger capabilities to migrate, and organisms basically escape the ocean motions by residing at the bottom. Thus, they can time the tidal phases and move to the bottom or other weaker current margins during unfavorable tidal current period and reenter the water column when currents switch to favorable directions (Cross et al., 2015; Forbes and Benfield, 1986). For estuaries with strong freshwater discharge, supposition of tide and riverine flow leads to different current velocities in space and time. The organisms can migrate within certain depth ranges to take advantage of maximizing landward or seaward transport during flood or ebb. This might be more common as weak swimming capabilities might be enough to reach favorable depth (Hobson and McQuoid, 2001; Jeannette, 2002).

Episodic events, such as typhoon, have differential impacts on different plankton groups (Grossmann et al., 2015). We observed an increase in chlorophyll *a* and a general negative impact on most plankton groups, but copepods. Many studies show increases in chlorophyll *a* concentrations and primary productivity after typhoon events (e.g., Chen et al., 2009; Lin, 2012; Wang, 2020). Impacts on zooplankton vary with potential benefit for carnivorous gelatinous zooplankton through resource pulse or transport accumulation (Kaneda et al., 2007; López-López et al., 2013). The positive response of copepods to typhoon events are likely related to changes in water masses, large freshwater impacts, and vertical migrations (Beyrend-Dur et al., 2013; Yang et al., 2019). The impacts appeared to vary with the strength of typhoon. Further studies are necessary to achieve a mechanistic understanding.

5.3. *Combining indicators for a better evaluation of ecosystem health*

Automated data streams from imaging systems opens the gate to further development of the existing indicators based on functional traits and much higher resolution. For example, the lifeform pair “gelatinous zooplankton and fish larvae” has been retained as an indicator of energy flow and possible trophic pathway, and to reflect changes in these dominant groups of zooplankton (Breitburg and Burrell, 2014; Purcell et al., 2001). The lifeform pair “Holoplankton and meroplankton” has been designed to provide information about the strength of benthic-pelagic coupling. The lifeform pair “phytoplankton and zooplankton abundance” provides an indication of changes in the transfer of energy from primary to secondary producers. A “large (>2mm) vs small copepods (<1.9mm)” is a size-based indicator of food web structure and energy flow efficiency through the food web (e.g., Bi et al., 2012b; Eisner et al., 2020; Hooff and Peterson, 2006).

The high-frequency time series of plankton indicators reflect the complexity of biotic and abiotic environments, and the intricacy of ecosystem functioning. The near real-time simultaneous measurements of plankton indicators can be integrated into an ecosystem-based management framework to evaluate ecosystem health (Rombouts et al., 2013; Tett et al., 2013). Many candidate indicators require monitoring across a continuum of spatial and temporal scales that is relevant for better understanding ecological processes (Kershner et al., 2011), and imaging systems can provide it. Community level indicators consisting of lower-trophic level, higher-productivity functional groups tend to be good indicators for ecosystem (Fulton, 2010; Samhouri et al., 2009; Trenkel and Rochet, 2003), and such information could be collected by an imaging system as Planktonscope.

Inconsistent sampling, data gaps and large variations in existing plankton data make it a tricky task to determine how indicators respond to environment forcing (Goberville et al., 2011; Southward et al., 1995), although it is essential to differentiate between natural and anthropogenic stress (Rombouts et al., 2013). High-frequency plankton indicators derived from imaging systems, in combination with a deep learning approach, provide consistent data and can capture the non-linear interactions between biology and the environment. Furthermore, the continuous high-frequency data flow can effectively capture the impacts of episodic ecological events or other dramatic changes in environmental conditions. The near real time measurements offer useful information for managers to act promptly before or when dramatic changes in ecosystems occur.

In situ plankton imaging systems like PlanktonScope significantly increase our ability to sample and monitor organisms in the pelagic realm. Recent advances in deep learning systems facilitate the deployment of in situ imaging systems and we expect a surge in the availability of high-frequency plankton data. The increase in frequency and resolution will lead to a better understanding of the interactions between organisms and their biotic and abiotic environments, while reducing the uncertainties due to insufficient sampling in traditional plankton surveys. The simultaneous measurements of a suite of plankton indicators can offer a near real-time holistic view of the pelagic ecosystem status. The availability of continuous near real-time data can support a much-needed foundation to improve the accuracies and predicting abilities of the existing IEA frameworks and the transition from hindsight to near real-time IEA.

Declaration of Competing Interest

The authors declare that they have no known competing financial interests or personal relationships that could have appeared to influence the work reported in this paper.

Data availability

Data will be made available on request.

References

Anderson, D.M., 2009. Approaches to monitoring, control and management of harmful algal blooms (HABs). Ocean Coast. Manag. 52, 342–347.
Attayde, J.L., Bozelli, R.L., 1998. Assessing the indicator properties of zooplankton assemblages to disturbance gradients by canonical correspondence analysis. Can. J. Fish. Aquat. Sci. 55, 1789–1797.
Aubry, A., Elliott, M., 2006. The use of environmental integrative indicators to assess seabed disturbance in estuaries and coasts: application to the Humber estuary, UK. Mar. Pollut. Bull. 53, 175–185.
Bakun, A., 1973. Coastal Upwelling Indices, West Coast of North America, 1946–71, NOAA Technical Report NMFS SSRF-671. National Marine Fisheries Service, p. 103.
Barbier, E.B., Hacker, S.D., Kennedy, C., Koch, E.W., Stier, A.C., Silliman, B.R., 2011. The value of estuarine and coastal ecosystem services. Ecol. Monogr. 81, 169–193.
Beardall, J., Allen, D., Bragg, J., Finkel, Z.V., Flynn, K.J., Quigg, A., Rees, T.A.V., Richardson, A.J., Raven, J.A., 2009. Allometry and stoichiometry of unicellular, colonial and multicellular phytoplankton. New Phytol. 181, 295–309.
Beaugrand, G., Kirby, R.R., 2010. Climate, plankton and cod. Glob. Chang. Biol. 16, 1268–1280.
Beaugrand, G., Edwards, M., Brander, K., Luczak, C., Ibanez, F., 2008. Causes and projections of abrupt climate-driven ecosystem shifts in the North Atlantic. Ecol. Lett. 11, 1157–1168.
Beaugrand, G., Conversi, A., Chiba, S., Edwards, M., Fonda-Umani, S., Greene, C., Mantua, N., Otto, S.A., Reid, P.C., Stachura, M.M., Stemmann, L., Sugisaki, H., 2015. Synchronous marine pelagic regime shifts in the northern hemisphere. Philosoph. Trans. Royal Soc. B: Biol. Sci. 370, 20130272.
Bedford, J., Johns, D., Greenstreet, S., McQuatters-Gollop, A., 2018. Plankton as prevailing conditions: a surveillance role for plankton indicators within the marine strategy framework directive. Mar. Policy 89, 109–115.
Bedford, J., Ostle, C., Johns, D.G., Budria, A., McQuatters-Gollop, A., 2020. The influence of temporal scale selection on pelagic habitat biodiversity indicators. Ecol. Indic. 114, 9.
Benfield, M.C., Grosjean, P., Culverhouse, P.F., Irigoien, X., Sieracki, M.E., Lopez-Urrutia, A., Dam, H.G., Hu, Q., Davis, C.S., Hansen, A., Pilskaln, C.H., Riseman, E.M., Schultz, H., Utgoff, P.E., Gorsky, G., 2007. RAPID: research on automated plankton identification. Oceanogr. 20, 172–187.

Beyrend-Dur, D., Souissi, S., Hwang, J.-S., 2013. Population dynamics of calanoid copepods in the subtropical mesohaline Danshuei estuary (Taiwan) and typhoon effects. Ecol. Res. 28, 771–780.
Bi, H., Ruppel, R.E., Peterson, W.T., Casillas, E., 2008. Spatial distribution of ocean habitat of yearling Chinook (*Oncorhynchus tshawytscha*) and coho (*Oncorhynchus kisutch*) salmon off Washington and Oregon, USA. Fish. Oceanogr. 17, 463–476.
Bi, H., Peterson, W.T., Lamb, J., Casilas, E., 2011a. Copepods and salmon: characterizing the spatial distribution of juvenile salmon along the Washington and Oregon coast, USA. Fish. Oceanogr. 20, 125–138.
Bi, H., Peterson, W.T., Strub, P.T., 2011b. Transport and coastal zooplankton communities in the northern California Current system. Geophys. Res. Lett. 38.
Bi, H., Cook, S., Yu, H., Benfield, M.C., Houde, E.D., 2012a. Deployment of an imaging system to investigate fine-scale spatial distribution of early life stages of the ctenophore *Mnemiopsis leidyi* in Chesapeake Bay. J. Plankton Res. 35, 270–280.
Bi, H., Peterson, W.T., Peterson, J.O., Fisher, J.L., 2012b. A comparative analysis of coastal and shelf-slope copepod communities in the northern California current system: synchronized response to large-scale forcing? Limnol. Oceanogr. 57, 1467–1478.
Bi, H., Ji, R., Liu, H., Jo, Y.-H., Hare, J.A., 2014. Decadal changes in zooplankton of the Northeast U.S. Continental Shelf. PLoS One 9, e87720.
Bi, H., Guo, Z., Benfield, M.C., Fan, C., Ford, M., Shahrestani, S., Sieracki, J.M., 2015. A semi-automated image analysis procedure for in ditu plankton imaging systems. PLoS One 10, e0127121.
Bi, H., Cheng, Y., Cheng, X., Benfield, M.C., Kimmel, D.G., Zheng, H., Groves, S., Ying, K., 2022. Taming the data deluge: a novel end-to-end deep learning framework for classifying marine biological and environmental images. IEEE Trans. Neural Netw. Learn. Syst. Submitted for publication.
Borja, A., Dauer, D.M., 2008. Assessing the environmental quality status in estuarine and coastal systems: comparing methodologies and indices. Ecol. Indic. 8, 331–337.
Borja, Á., Dauer, D.M., Elliott, M., Simenstad, C.A., 2010. Medium- and long-term recovery of estuarine and coastal ecosystems: patterns, rates and restoration effectiveness. Estuar. Coasts 33, 1249–1260.
Breitburg, D., Burrell, R., 2014. Predator-mediated landscape structure: seasonal patterns of spatial expansion and prey control by *Chrysaora quinquecirrha* and *Mnemiopsis leidyi*. Mar. Ecol.-Prog. Ser. 510, 183–200.
Breton, E., Christaki, U., Sautour, B., Demonio, O., Skouroliakou, D.-I., Beaugrand, G., Seuront, L., Kléparski, L., Poquet, A., Nowaczyk, A., Crouvoisier, M., Ferreira, S., Pecqueur, D., Salmeron, C., Brylinski, J.-M., Lheureux, A., Goberville, E., 2021. Seasonal variations in the biodiversity, ecological strategy, and specialization of diatoms and copepods in a coastal system with phaeocystis blooms: the key role of trait trade-offs. Front. Mar. Sci. 8.
Burckle, L.H., Haq, B.U., 1998. Marine diatoms. In: Boersma, A. (Ed.), Introduction Tomarine Micropaleontology. Elsevier Science B.V., Amsterdam, pp. 245–266.
Campbell, R.W., Roberts, P.L., Jaffe, J., 2020. The Prince William sound plankton camera: a profiling in situ observatory of plankton and particulates. ICES J. Mar. Sci. 77, 1440–1455.
Chen, Y.L.L., Chen, H.Y., Jan, S., Tuo, S.H., 2009. Phytoplankton productivity enhancement and assemblage change in the upstream Kuroshio after typhoons. Mar. Ecol.-Prog. Ser. 385, 111–126.
Chen, Z., Gong, W., Cai, H., Chen, Y., Zhang, H., 2017. Dispersal of the Pearl River plume over continental shelf in summer. Estuar. Coast. Shelf Sci. 194, 252–262.
Cheng, K., Cheng, X., Wang, Y., Bi, H., Benfield, M.C., 2019. Enhanced convolutional neural network for plankton identification and enumeration. PLoS One 14, e0219570.
Cheng, X., Cheng, K., Bi, H., 2020. Dynamic downscaling S=-segmentation for noisy, low-contrast in situ underwater plankton images. IEEE Access 8, 111012–111026.
Clancy, M., Cobb, J.S., 1997. Effect of wind and tidal advection on distribution patterns of rock crab *Cancer irroratus* megalopae in Block Island sound, Rhode Island. Mar. Ecol.-Prog. Ser. 152, 217–225.
Corgnati, L., Marini, S., Mazzei, L., Ottaviani, E., Aliani, S., Conversi, A., Griffa, A., 2016. Looking inside the ocean: toward an autonomous imaging system for monitoring gelatinous zooplankton. Sensors 16, 2124.
Cowen, R.K., Guigand, C.M., 2008. In situ ichthyoplankton imaging system (ISIIS): system design and preliminary results. Limnol. Oceanogr. Methods 6, 126–132.
Cowen, R.K., Sponaugle, S., 2009. Larval dispersal and marine population connectivity. Annu. Rev. Mar. Sci. 1, 443–466.
Cresswell, G.R., 2000. Coastal currents of northern Papua New Guinea, and the Sepik River outflow. Mar. Freshw. Res. 51, 553–564.
Cross, J., Nimmo-Smith, W.A.M., Hosegood, P.J., Torres, R., 2015. The role of advection in the distribution of plankton populations at a moored 1-D coastal observatory. Prog. Oceanogr. 137, 342–359.
Cushing, D.H., 1969. The regularity of the spawning season of some fishes. ICES J. Mar. Sci. 33, 81–92.
Daly, K.L., Smith, W.O., 1993. Physical-biological interactions influencing marine plankton production. Annu. Rev. Ecol. Syst. 24, 555–585.
Davis, C., Gallager, S., Berman, M., Haury, L., Strickler, J., 1992. The video plankton recorder (VPR): design and initial results. Arch. Hydrobiol. Beih. 36, 67–81.
Dickey, T., Zedler, S., Yu, X., Doney, S.C., Frye, D., Jannasch, H., Manov, D., Sigurdson, D., McNeil, J.D., Dobeck, L., Gilboy, T., Bravo, C., Siegel, D.A., Nelson, N., 2001. Physical and biogeochemical variability from hours to years at the Bermuda testbed mooring site: June 1994–March 1998. Deep Sea Res. Pt II 48, 2105–2140.
Diekmann, R., Möllmann, C., Bergström, L., Flinkman, J., Gårdmark, A., Kornilovs, G., Lindegren, M., MüllerKarulis, B., Plikshs, N., Põllumäe, A., 2010. Integrated ecosystem assessments of seven Baltic Sea areas covering the last three decades. In: Diekmann, R., Möllmann, C. (Eds.), ICES Coooperative Research Report No. 302. International Council for the Exploration of the Sea, Denmark, p. 90.
Ding, Y., Chan, J.C.L., 2005. The east Asian summer monsoon: an overview. Meteorol. Atmospheric Phys. 89, 117–142.
Doney, S., Sailley, S., 2013. When an ecological regime shift is really just stochastic noise. In: Proc. Nat. Acad. Sci. U. S. A, p. 110.
Druon, J.-N., Hélaouët, P., Beaugrand, G., Fromentin, J.-M., Palialexis, A., Hoepffner, N., 2019. Satellite-based indicator of zooplankton distribution for global monitoring. Sci. Rep. 9, 4732.
Dumelle, M., Lamb, J.F., Jacobson, K.C., Hunsicker, M., Morgan, C.A., Burke, B.J., Peterson, W.T., 2021. Capturing copepod dynamics in the northern California current using sentinel stations. Prog. Oceanogr. 193, 102550.
Eisner, L.B., Yasumiishi, E.M., Andrews, A.G., O'Leary, C.A., 2020. Large copepods as leading indicators of walleye Pollock recruitment in the southeastern Bering Sea: sample-based and spatio-temporal model (VAST) results. Fish. Res. 232, 14.
Feyrer, L.J., Duffus, D.A., 2015. Threshold foraging by gray whales in response to fine scale variations in mysid density. Mar. Mamm. Sci. 31, 560–578.
Forbes, A.T., Benfield, M.C., 1986. Tidal behaviour of post-larval penaeid prawns (*Crustacea: Decapoda: Penaeidae)* in a southeast African estuary. J. Exp. Mar. Biol. Ecol. 102, 23–34.
Fulton, E.A., 2010. Approaches to end-to-end ecosystem models. J. Mar. Syst. 81, 171–183.
Gan, J., Lu, Z., Cheung, A., Dai, M., Liang, L., Harrison, P.J., Zhao, X., 2014. Assessing ecosystem response to phosphorus and nitrogen limitation in the Pearl River plume using the Regional Ocean modeling system (ROMS). J. Geophys. Res. Oceans 119, 8858–8877.
Gao, S., Hjøllo, S.S., Falkenhaug, T., Strand, E., Edwards, M., Skogen, M.D., 2021. Overwintering distribution, inflow patterns and sustainability of *Calanus finmarchicus* in the North Sea. Prog. Oceanogr. 194, 102567.
Goberville, E., Beaugrand, G., Sautour, B., Tréguer, P., 2011. Evaluation of coastal perturbations: a new mathematical procedure to detect changes in the reference state of coastal systems. Ecol. Indic. 11, 1290–1300.
Gong, Y.X. Yayuan, Xu, Shannan, Liu, Yong, Yang, Yutao, Huang, Zirong, Li, Chunhou, 2019. Zooplankton community structure in Hailing Bay and its relationship with primary environmental factors. South China Fish. Sci. 15, 49–55.
Grossmann, M.M., Gallager, S.M., Mitarai, S., 2015. Continuous monitoring of near-bottom mesoplankton communities in the East China Sea during a series of typhoons. J. Oceanogr. 71, 115–124.
Guan, B., 1978. The warm current in the South China Sea - a current flowing against the wind in winter in the open sea off Guangdong Province. Oceanol. Limnol. Sin. 9, 117–127.
Gui, J., Wei, Y., Sun, J., Le, F., Cai, Y., Ning, X., 2020. Summer phytoplankton assemblages and carbon biomass in the northern South China Sea. Cont. Shelf Res. 210, 104276.
Halpern, B.S., Walbridge, S., Selkoe, K.A., Kappel, C.V., Micheli, F., D'Agrosa, C., Bruno, J.F., Casey, K.S., Ebert, C., Fox, H.E., Fujita, R., Heinemann, D., Lenihan, H.S., Madin, E.M.P., Perry, M.T., Selig, E.R., Spalding, M., Steneck, R., Watson, R., 2008. A global map of human impact on marine ecosystems. Science 319, 948–952.
Harvey, C.J., Fisher, J.L., Samhouri, J.F., Williams, G.D., Francis, T.B., Jacobson, K.C., deReynier, Y.L., Hunsicker, M.E., Garfield, N., 2020. The importance of long-term ecological time series for integrated ecosystem assessment and ecosystem-based management. Prog. Oceanogr. 188, 102418.
Heath, M.R., Lough, R.G., 2007. A synthesis of large-scale patterns in the planktonic prey of larval and juvenile cod (*Gadus morhua*). Fish. Oceanogr. 16, 169–185.
Helaouët, P., Beaugrand, G., 2007. Macroecology of *Calanus finmarchicus* and *C. helgolandicus* in the North Atlantic Ocean and adjacent seas. Mar. Ecol.-Prog. Ser. 345, 147–165.
Heneghan, R.F., Everett, J.D., Sykes, P., Batten, S.D., Edwards, M., Takahashi, K., Suthers, I.M., Blanchard, J.L., Richardson, A.J., 2020. A functional size-spectrum model of the global marine ecosystem that resolves zooplankton composition. Ecol. Model. 435, 109265.
Hjort, J., 1914. Fluctuations in the great fisheries of northern Europe viewed in the light of biological research. J. Cons. Int. Explor. Mer 20, 1–228.
Hobson, L.A., McQuoid, M.R., 2001. Pelagic diatom assemblages are good indicators of mixed water intrusions into Saanich inlet, a stratified fjord in Vancouver Island. Mar. Geol. 174, 125–138.
Hooff, R.C., Peterson, W.T., 2006. Copepod biodiversity as an indicator of changes in ocean and climate conditions of the northern California current ecosystem. Limnol. Oceanogr. 51, 2607–2620.
Hosia, A., Falkenhaug, T., Baxter, E.J., Pagès, F., 2017. Abundance, distribution and diversity of gelatinous predators along the northern mid-Atlantic ridge: a comparison of different sampling methodologies. PLoS One 12, e0187491.
Huserbråten, M.B.O., Moland, E., Albretsen, J., 2018. Cod at drift in the North Sea. Prog. Oceanogr. 167, 116–124.
Irisson, J.-O., Ayata, S.-D., Lindsay, D.J., Karp-Boss, L., Stemmann, L., 2022. Machine learning for the study of plankton and marine snow from images. Annu. Rev. Mar. Sci. 14, 277–301.
Jeannette, E.Z., 2002. Tidal changes in copepod abundance and maintenance of a summer Coscinodiscus bloom in the southern San Juan Channel, San Juan Islands, USA. Mar. Ecol.-Prog. Ser. 226, 193–210.
Jiao, W., X, C, Hu, Y., Hao, Q., Bi, H., 2022. Image recognition based on compressive imaging and optimal feature selection. IEEE Photonics J. 14, 1–12.
Kaneda, A., Kohama, T., Kawamura, Y., Takeoka, H., 2007. Periodicity in the accumulation of gelatinous zooplankton during the summer season in the coastal area of Iyo-Nada, Japan. Limnol. Oceanogr. 52, 707–715.
Keister, J.E., Di Lorenzo, E., Morgan, C.A., Combes, V., Peterson, W.T., 2011. Zooplankton species composition is linked to ocean transport in the northern California current. Glob. Chang. Biol. 17, 2498–2511.

Kershner, J., Samhouri, J.F., James, C.A., Levin, P.S., 2011. Selecting indicator portfolios for marine species and food webs: a Puget Sound case study. PLoS One 6, e25248.
Kim, J.-S., Zhou, W., Cheung, H.N., Chow, C.H., 2013. Variability and risk analysis of Hong Kong air quality based on monsoon and El Niño conditions. Adv. Atmos. Sci. 30, 280–290.
Kleinbaum, D.G., Dietz, K., Gail, M., Klein, M., Klein, M., 2002. Logistic Regression: A Self-Learning Text. Springer, New York, NY.
Knapp, K.R., Diamond, H.J., Kossin, J.P., Kruk, M.C., Schreck, C., 2018. International Best Track Archive for Climate Stewardship (IBTrACS) Project, Version 4. NOAA National Centers for Environmental Information.
Lebrato, M., Pahlow, M., Frost, J.R., Küter, M., de Jesus Mendes, P., Molinero, J.-C., Oschlies, A., 2019. Sinking of gelatinous zooplankton biomass increases deep carbon transfer efficiency globally. Glob. Biogeochem. Cycles 33, 1764–1783.
Levin, P.S., Fogarty, M.J., Murawski, S.A., Fluharty, D., 2009. Integrated ecosystem assessments: developing the scientific basis for ecosystem-based management of the ocean. PLoS Biol. 7, e1000014.
Lin, I.-I., 2012. Typhoon-induced phytoplankton blooms and primary productivity increase in the western North Pacific subtropical ocean. J. Geophys. Res. Oceans 117.
Litchman, E., Klausmeier, C.A., Schofield, O.M., Falkowski, P.G., 2007. The role of functional traits and trade-offs in structuring phytoplankton communities: scaling from cellular to ecosystem level. Ecol. Lett. 10, 1170–1181.
Liu, H., Bi, H., Peterson, W.T., 2015. Large-scale forcing of environmental conditions on subarctic copepods in the northern California current system. Prog. Oceanogr. 134, 404–412.
Liu, D.Y., Kezhen, Cai, Zhonghua, Huang, Honghui, Bi, Hongsheng, 2021. Outburst of *Creseis acicula* in southwest Daya bay in July 2020. Oceanol. Limnol. Sin. 52, 1438–1447.
Lomartire, S., Marques, J.C., Gonçalves, A.M.M., 2021. The key role of zooplankton in ecosystem services: a perspective of interaction between zooplankton and fish recruitment. Ecol. Indic. 129, 107867.
López-López, L., Molinero, J.C., Tseng, L.-C., Chen, Q.-C., Hwang, J.-S., 2013. Seasonal variability of the gelatinous carnivore zooplankton community in northern Taiwan. J. Plankton Res. 35, 677–683.
Lotze, H.K., Lenihan, H.S., Bourque, B.J., Bradbury, R.H., Cooke, R.G., Kay, M.C., Kidwell, S.M., Kirby, M.X., Peterson, C.H., Jackson, J.B.C., 2006. Depletion, gegradation, and recovery potential of estuaries and coastal seas. Science 312, 1806–1809.
Luo, J.Y., Irisson, J.-O., Graham, B., Guigand, C., Sarafraz, A., Mader, C., Cowen, R.K., 2018. Automated plankton image analysis using convolutional neural networks. Limnol. Oceanogr. Methods 16, 814–827.
Mackas, D.L., Beaugrand, G., 2010. Comparisons of zooplankton time series. J. Mar. Syst. 79, 286–304.
Mackas, D.L., Denman, K.L., Abbott, M.R., 1985. Plankton patchiness: biology in the physical vernacular. Bull. Mar. Sci. 37, 652–674.
Mackas, D.L., Thomson, R.E., Galbraith, M., 2001. Changes in the zooplankton community of the British Columbia continental margin, 1985-1999, and their covariation with oceanographic conditions. Can. J. Fish. Aquat. Sci. 58, 685–702.
Marcot, J., 1976. Marine plankton diatoms as indicators of ocean ciculation in Bay of Bengal. Bot. Mar. 19, 189–194.
McGowan, J.A., Walker, P.W., 1979. Structure in the copepod community of the North Pacific central gyre. Ecol. Monogr. 49, 195–226.
McManus, M.A., Woodson, C.B., 2012. Plankton distribution and ocean dispersal. J. Exp. Biol. 215, 1008–1016.
Melbourne-Thomas, J., 2020. Climate shifts for krill predators. Nat. Clim. Chang. 10, 390–391.
Merz, E., Kozakiewicz, T., Reyes, M., Ebi, C., Isles, P., Baity-Jesi, M., Roberts, P., Jaffe, J. S., Dennis, S.R., Hardeman, T., Stevens, N., Lorimer, T., Pomati, F., 2021. Underwater dual-magnification imaging for automated lake plankton monitoring. Water Res. 203, 117524.
Mills, C.E., 2001. Jellyfish blooms: are populations increasing globally in response to changing ocean conditions? Hydrobiologia 451, 55–68.
Möller, K.O., St John, M., Temming, A., Floeter, J., Sell, A.F., Herrmann, J.P., Möllmann, C., 2012. Marine snow, zooplankton and thin layers: indications of a trophic link from small-scale sampling with the video plankton recorder. Mar. Ecol.-Prog. Ser. 468, 57–69.
Möller, K.O., St John, M., Temming, A., Diekmann, R., Peters, J., Floeter, J., Sell, A.F., Herrmann, J.-P., Gloe, D., Schmidt, J.O., Hinrichsen, H.H., MÖllmann, C., 2020. Predation risk triggers copepod small-scale behavior in the Baltic Sea. J. Plankton Res. 42, 702–713.
Nagelkerken, I., Sheaves, M., Baker, R., Connolly, R.M., 2015. The seascape nursery: a novel spatial approach to identify and manage nurseries for coastal marine fauna. Fish Fish. 16, 362–371.
Ndah, A.B., Meunier, C.L., Kirstein, I.V., Gobel, J., Ronn, L., Boersma, M., 2022. A systematic study of zooplankton-based indices of marine ecological change and water quality: application to the European marine strategy framework directive (MSFD). Ecol. Indic. 135, 15.
Olson, R.J., Sosik, H.M., 2007. A submersible imaging-in-flow instrument to analyze nano-and microplankton: imaging FlowCytobot. Limnol. Oceanogr. Methods 5, 195–203.
Orenstein, E.C., Ratelle, D., Briseño-Avena, C., Carter, M.L., Franks, P.J.S., Jaffe, J.S., Roberts, P.L.D., 2020. The Scripps plankton camera system: a framework and platform for in situ microscopy. Limnol. Oceanogr. Methods 18, 681–695.
Orenstein, E.C., Ayata, S.-D., Maps, F., Becker, É.C., Benedetti, F., Biard, T., de Garidel-Thoron, T., Ellen, J.S., Ferrario, F., Giering, S.L.C., Guy-Haim, T., Hoebeke, L., Iversen, M.H., Kiørboe, T., Lalonde, J.-F., Lana, A., Laviale, M., Lombard, F., Lorimer, T., Martini, S., Meyer, A., Möller, K.O., Niehoff, B., Ohman, M.D., Pradalier, C., Romagnan, J.-B., Schröder, S.-M., Sonnet, V., Sosik, H.M., Stemmann, L.S., Stock, M., Terbiyik-Kurt, T., Valcárcel-Pérez, N., Vilgrain, L., Wacquet, G., Waite, A.M., Irisson, J.-O., 2022. Machine learning techniques to characterize functional traits of plankton from image data. Limnol. Oceanogr. 67, 1647–1669.
Papworth, D.J., Marini, S., Conversi, A., 2016. A novel, unbiased analysis approach for investigating population dynamics: a case study on *Calanus finmarchicus* and its decline in the North Sea. PLoS One 11, e0158230.
Picheral, M., Guidi, L., Stemmann, L., Karl, D.M., Iddaoud, G., Gorsky, G., 2010. The underwater vision profiler 5: an advanced instrument for high spatial resolution studies of particle size spectra and zooplankton. Limnol. Oceanogr. Methods 8, 462–473.
Piet, G.J., Jansen, H.M., Rochet, M.-J., 2008. Evaluating potential indicators for an ecosystem approach to fishery management in European waters. ICES J. Mar. Sci. 65, 1449–1455.
Pineda, J., 1991. Predictable upwelling and the shoreward transport of planktonic larvae by internal tidal bores. Science 253, 548–549.
Purcell, J.E., 1985. Predation on fish eggs and larvae by pelagic cnidarians and ctenophores. Bull. Mar. Sci. 37, 739–755.
Purcell, J.E., Malej, A., Benović, A., 1999. Potential links of jellyfish to eutrophication and fisheries, ecosystems at the land-sea margin: drainage basin to coastal sea, pp. 241–263.
Purcell, J.E., Breitburg, D.L., Decker, M.B., Graham, W.M., Youngbluth, M.J., Raskoff, K. A., 2001. Pelagic cnidarians and ctenophores in low dissolved oxygen environments: a review. Coast. Estuar. Stud. 77–100.
Purcell, J.E., Uye, S., Lo, W., 2007. Anthropogenic causes of jellyfish blooms and their direct consequences for humans: a review. Mar. Ecol.-Prog. Ser. 350, 153–174.
Racault, M.-F., Le Quéré, C., Buitenhuis, E., Sathyendranath, S., Platt, T., 2012. Phytoplankton phenology in the global ocean. Ecol. Indic. 14, 152–163.
Racault, M.-F., Platt, T., Sathyendranath, S., Ağirbaş, E., Martinez Vicente, V., Brewin, R., 2014. Plankton indicators and ocean observing systems: support to the marine ecosystem state assessment. J. Plankton Res. 36, 621–629.
Reid, J.L., Brinton, E., Fleminger, A., Venrick, E.L., McGowan, J.A., 1978. Ocean circulation and marine life. In: Charnock, H., Deacon, G. (Eds.), Advances in Oceanography. Springer, US, Boston, MA, pp. 65–130.
Richardson, A.J., Bakun, A., Hays, G.C., Gibbons, M.J., 2009. The jellyfish joyride: causes, consequences and management responses to a more gelatinous future. Trends Ecol. Evol. 24, 312–322.
Roemmich, D., McGowan, J., 1995. Climatic warming and the decline of zooplankton in the California current. Science 267, 1324–1326.
Romagnan, J.B., Aldamman, L., Gasparini, S., Nival, P., Aubert, A., Jamet, J.L., Stemmann, L., 2016. High frequency mesozooplankton monitoring: can imaging systems and automated sample analysis help us describe and interpret changes in zooplankton community composition and size structure - an example from a coastal site. J. Mar. Syst. 162, 18–28.
Rombouts, I., Beaugrand, G., Artigas, L.F., Dauvin, J.C., Gevaert, F., Goberville, E., Kopp, D., Lefebvre, S., Luczak, C., Spilmont, N., Travers-Trolet, M., Villanueva, M.C., Kirby, R.R., 2013. Evaluating marine ecosystem health: case studies of indicators using direct observations and modelling methods. Ecol. Indic. 24, 353–365.
Rutten, T.P.A., Sandee, B., Hofman, A.R.T., 2005. Phytoplankton monitoring by high performance flow cytometry: a successful approach? Cytometry A 64A, 16–26.
Samhouri, J.F., Levin, P.S., Harvey, C.J., 2009. Quantitative evaluation of marine ecosystem indicator performance using food web models. Ecosyst. 12, 1283–1298.
Schindler, D.W., 1998. Whole-ecosystem experiments: eeplication versus realism: the need for ecosystem-scale experiments. Ecosyst. 1, 323–334.
Serranito, B., Aubert, A., Stemmann, L., Rossi, N., Jamet, J.L., 2016. Proposition of indicators of anthropogenic pressure in the bay of Toulon (Mediterranean Sea) based on zooplankton time-series. Cont. Shelf Res. 121, 3–12.
Sheaves, M., Baker, R., Nagelkerken, I., Connolly, R.M., 2015. True value of estuarine and coastal nurseries for fish: incorporating complexity and dynamics. Estuar. Coasts 38, 401–414.
Shin, Y.-J., Shannon, L.J., Bundy, A., Coll, M., Aydin, K., Bez, N., Blanchard, J.L., Borges, M.D.F., Diallo, I., Diaz, E., Heymans, J.J., Hill, L., Johannesen, E., Jouffre, D., Kifani, S., Labrosse, P., Link, J.S., Mackinson, S., Masski, H., Möllmann, C., Neira, S., Ojaveer, H., Ould Mohammed Abdallahi, K., Perry, I., Thiao, D., Yemane, D., Cury, P. M., 2010. Using indicators for evaluating, comparing, and communicating the ecological status of exploited marine ecosystems. 2. Setting the scene. ICES J. Mar. Sci. 67, 692–716.
Show, I.T., 1980. The movements of a marine copepod in a tidal lagoon. In: Hamilton, P., Macdonald, K.B. (Eds.), Estuarine and Wetland Processes: With Emphasis on Modeling. Springer US, Boston, MA, pp. 561–601.
Song, J., Bi, H., Cai, Z., Cheng, X., He, Y., Benfield, M.C., Fan, C., 2020. Early warning of *Noctiluca scintillans* blooms using in-situ plankton imaging system: an example from Dapeng Bay, P.R. China. Ecol. Indic. 112, 106123.
Song, J., Jiao, W., Lankowicz, K., Cai, Z., Bi, H., 2022. A two-stage adaptive thresholding segmentation for noisy low-contrast images. Ecol. Inform. 69, 101632.
Southward, A.J., Hawkins, S.J., Burrows, M.T., 1995. Seventy years' observations of changes in distribution and abundance of zooplankton and intertidal organisms in the western English Channel in relation to rising sea temperature. J. Therm. Biol. 20, 127–155.
Teodósio, M.A., Barbosa, A.M.B., 2022. Zooplankton Ecology. CRC Press.
Tett, P., Gowen, R.J., Painting, S.J., Elliott, M., Forster, R., Mills, D.K., Bresnan, E., Capuzzo, E., Fernandes, T.F., Foden, J., Geider, R.J., Gilpin, L.C., Huxham, M., McQuatters-Gollop, A.L., Malcolm, S.J., Saux-Picart, S., Platt, T., Racault, M.F.,

Sathyendranath, S., van der Molen, J., Wilkinson, M., 2013. Framework for understanding marine ecosystem health. Mar. Ecol.-Prog. Ser. 494, 1–27.
Tinta, T., Klun, K., Herndl, G.J., 2021. The importance of jellyfish–microbe interactions for biogeochemical cycles in the ocean. Limnol. Oceanogr. 66, 2011–2032.
Torrence, C., Compo, G.P., 1998. A practical guide to wavelet analysis. Bull. Amer. Meteor. 79, 61–78.
Trathan, P.N., Hill, S.L., 2016. The importance of krill predation in the Southern Ocean. In: Siegel, V. (Ed.), Biology and Ecology of Antarctic Krill. Springer International Publishing, Cham, pp. 321–350.
Trenkel, V.M., Rochet, M.-J., 2003. Performance of indicators derived from abundance estimates for detecting the impact of fishing on a fish community. Can. J. Fish. Aquat. Sci. 60, 67–85.
Trevorrow, M.V., Mackas, D.L., Benfield, M.C., 2005. Comparison of multifrequency acoustic and in situ measurements of zooplankton abundances in knight inlet, British Columbia. J. Acoust. Soc. Am. 117, 3574–3588.
Tung, Y.-S., Wang, S.-Y.S., Chu, J.-L., Wu, C.-H., Chen, Y.-M., Cheng, C.-T., Lin, L.-Y., 2020. Projected increase of the East Asian summer monsoon (Meiyu) in Taiwan by climate models with variable performance. Meteorol. Appl. 27, e1886.
Uye, S.-I., 2014. The Giant jellyfish Nemopilema nomurai in East Asian marginal seas. In: Pitt, K.A., Lucas, C.H. (Eds.), Jellyfish Blooms. Springer, Netherlands, Dordrecht, pp. 185–205.
Wang, Y., 2020. Composite of typhoon-Induced Sea surface temperature and chlorophyll-a responses in the South China Sea. J. Geophys. Res. Oceans 125, e2020JC016243.
Winder, M., Sommer, U., 2012. Phytoplankton response to a changing climate. Hydrobiologia 698, 5–16.
Wu, N., Faber, C., Sun, X., Qu, Y., Wang, C., Ivetic, S., Riis, T., Ulrich, U., Fohrer, N., 2016. Importance of sampling frequency when collecting diatoms. Sci. Rep. 6, 36950.
Xie, M., Yao, S., Li, W., Zhao, H., Gao, Z., 2015. Investigation of the movement characteristics of West Guangdong longshore ocean current system, China. J. Coast. Res. 364–368.
Yang, C., Xu, D., Chen, Z., Wang, J., Xu, M., Yuan, Y., Zhou, M., 2019. Diel vertical migration of zooplankton and micronekton on the northern slope of the South China Sea observed by a moored ADCP. Deep Sea Res. Pt II. 167, 93–104.
Zhou, W.H., Xiaodan, Huang, Zhong, Xiao, Weijun, 2008. The characteristic of sea-land breeze in Yangjiang area and its impact on precipitation and temperature. Meteorol. Monogr. 34, 44–53.